

**Modelling tropical
tracer transport**

C. R. Hoyle et al.

This discussion paper is/has been under review for the journal Atmospheric Chemistry and Physics (ACP). Please refer to the corresponding final paper in ACP if available.

Tropical deep convection and its impact on composition in global and mesoscale models – Part 2: Tracer transport

C. R. Hoyle^{1,2}, V. Marécal⁷, M. R. Russo⁹, J. Arteta⁶, C. Chemel⁴,
M. P. Chipperfield³, F. D'Amato¹³, O. Dessens¹², W. Feng³, N. R. P. Harris¹¹,
J. S. Hosking^{12,*}, O. Morgenstern^{5,**}, T. Peter¹, J. A. Pyle⁹, T. Reddman¹⁰,
N. A. D. Richards³, P. J. Telford¹¹, W. Tian³, S. Viciani¹⁴, O. Wild⁸, X. Yang¹², and
G. Zeng⁵

¹Institute for Atmospheric and Climate Science, ETH Zurich, Zurich, Switzerland

²Department of Geosciences, University of Oslo, Norway

³Institute for Climate and Atmospheric Science, School of Earth and Environment, University of Leeds, UK

⁴NCAS-Weather, Centre for Atmospheric & Instrumentation Research, University of Herfordshire, UK

⁵NCAS-Chemistry Climate, Department of Chemistry, Cambridge University, UK

Title Page

Abstract

Introduction

Conclusions

References

Tables

Figures

◀

▶

◀

▶

Back

Close

Full Screen / Esc

Printer-friendly Version

Interactive Discussion



Modelling tropical tracer transport

C. R. Hoyle et al.

Title Page

Abstract

Introduction

Conclusions

References

Tables

Figures

I◀

▶I

◀

▶

Back

Close

Full Screen / Esc

Printer-friendly Version

Interactive Discussion



⁶Centre National de Recherches Météorologiques/Groupe d'étude de l'Atmosphère Météorologique, Météo-France and CNRS, Toulouse, France

⁷Laboratoire de Physique et Chimie de l'Environnement et de l'Espace, CNRS and University of Orléans, Orléans, France

⁸Lancaster Environment Centre, Lancaster University, UK

⁹NCAS climate, Centre for Atmospheric Science, Department of Chemistry, University of Cambridge, UK

¹⁰Institute for Meteorology and Climate Research, Karlsruhe Institute of Technology, Karlsruhe, Germany

¹¹European Ozone Research Coordinating Unit, University of Cambridge Department of Chemistry, Lensfield Road, Cambridge CB2 1EW, UK

¹²Centre for Atmospheric Science, University of Cambridge, Cambridge, UK

¹³CNR-INO (Istituto Nazionale di Ottica) Largo E. Fermi, 6 50125 Firenze, Italy

*now at: British Antarctic Survey, Cambridge, UK

**now at: the National Institute of Water and Atmospheric Research, Lauder, New Zealand

Received: 5 July 2010 – Accepted: 24 August 2010 – Published: 27 August 2010

Correspondence to: C. R. Hoyle (christopher.hoyle@env.ethz.ch)

Published by Copernicus Publications on behalf of the European Geosciences Union.

Abstract

The tropical transport processes of 14 different models or model versions were compared, within the framework of the SCOUT-O3 (Stratospheric-Climatic Links with Emphasis on the Upper Troposphere and Lower Stratosphere) project. The tested models range from the regional to the global scale, and include numerical weather prediction (NWP), chemistry transport, and climate chemistry models. Idealised tracers were used in order to prevent the model's chemistry schemes from influencing the results substantially, so that the effects of modelled transport could be isolated. We find large differences in the vertical transport of very short lived tracers (with a lifetime of 6 hours) within the tropical troposphere. Peak convective outflow altitudes range from around 300 hPa to almost 100 hPa among the different models, and the upper tropospheric tracer mixing ratios differ by up to an order of magnitude. The timing of convective events is found to differ between the models, even among those which source their forcing data from the same NWP model (ECMWF). The differences are less pronounced for longer lived tracers, however they could have implications for the modelling of the halogen burden of the lowermost stratosphere through species such as bromoform, or for the transport of short lived hydrocarbons into the lowermost stratosphere. The modelled tracer profiles are found to be strongly influenced by the convective transport parameterisations, and boundary layer mixing parameterisations of the models. The location of rapid transport into the upper troposphere is similar among the models, and is mostly concentrated over the western Pacific, the Maritime Continent and the Indian Ocean. In contrast, none of the models indicates significant enhancement in upward transport over western Africa. The mean mixing ratios of an idealised CO like tracer in the upper tropical troposphere are found to be sensitive to the surface CO mixing ratios in the regions with the most active convection, revealing the importance of correctly modelling both the location of convective transport and the geographical pollutant emission patterns.

Modelling tropical tracer transport

C. R. Hoyle et al.

Title Page

Abstract

Introduction

Conclusions

References

Tables

Figures

◀

▶

◀

▶

Back

Close

Full Screen / Esc

Printer-friendly Version

Interactive Discussion



1 Introduction

The time scales for atmospheric transport and photochemical production/loss are critical, interlinked factors in determining the distribution of trace species in the atmosphere. Short-lived chemical species emitted at the Earth's surface are removed in the lower troposphere unless they encounter meteorological conditions that result in fast upward transport to the upper troposphere or lower stratosphere (UT/LS). In the tropics the main meteorological phenomena in which this occurs are individual thunderstorms and larger areas of convection. The quantity of short-lived species which reaches the UT/LS in the tropics is not known with great confidence from either observational or modelling studies (Law and Sturges, 2007). Recently the issue has received greater attention as the potential role of very short-lived halocarbons in the bromine budget and in stratospheric ozone depletion has been recognised (e.g. Sturges et al., 2000; Salawitch et al., 2005; Sinnhuber and Folkins, 2006; Feng et al., 2007; Laube et al., 2008; Hossaini et al., 2010; Liang et al., 2010). In addition, fast transport is important in determining the atmospheric distributions of other natural, short-lived species (e.g. hydrocarbons and their breakdown products) as well as anthropogenic pollutants such as CO, C₂H₂ (Park et al., 2008) and, by implication, NO_x. Their fate, once in the UT/LS, is determined to a large extent by the altitude to which they are lofted.

In considering just the short-lived halocarbons such as bromoform and dibromomethane, which are likely to provide some, if not all of the reported "missing" bromine in the stratospheric bromine budget, one needs to know the amount of bromine in these gases which is lofted to a region of upward motion (Sinnhuber and Folkins, 2006).

In the tropics there is a gradual transition from tropospheric to stratospheric behaviour known as the tropical tropopause layer (TTL) (e.g. Fueglistaler et al., 2009, and references therein). Net upward motion occurs above the level of zero radiative heating, which is where radiative heating becomes positive and air rises. The exact level where this takes place depends on the local temperature profile, the water vapour

Modelling tropical tracer transport

C. R. Hoyle et al.

Title Page

Abstract

Introduction

Conclusions

References

Tables

Figures

◀

▶

◀

▶

Back

Close

Full Screen / Esc

Printer-friendly Version

Interactive Discussion



Modelling tropical tracer transport

C. R. Hoyle et al.

Title Page

Abstract

Introduction

Conclusions

References

Tables

Figures

◀

▶

◀

▶

Back

Close

Full Screen / Esc

Printer-friendly Version

Interactive Discussion



mixing ratio and whether or not clouds are present (e.g. Hartmann and Larson, 2002; Corti et al., 2005). A typical value is 15 km (ca. 120 hPa) (Sherwood and Dessler, 2000), which is above the level of maximum convective outflow (about 12–13 km, or 195–165 hPa) (Folkins et al., 1999, 2000). As a result, only a fraction of the air lofted up in convective flow reaches this higher level, and so any studies considering how much of this lofted air eventually reaches the stratosphere have to consider the tail in the distribution of convective outflow. This is not well known from either observational or modelling studies, and there has recently been considerable controversy on this matter (e.g. Kupper et al., 2004; Ricaud et al., 2007; Fueglistaler et al., 2009).

A number of studies have investigated the mass transported and altitude reached by convective transport, using different models and parameterisations. Folkins et al. (2006) compared two convective parameterisations in a one-dimensional framework as well as two further parameterisations in the GEOS-3 and GEOS-4 global models, with climatologies of CO, H₂O, HNO₃ and O₃, and found that the models which produce a more clearly defined convective outflow layer in the region of 10–13 km (or ca. 265–165 hPa) altitude matched the measurements best. Arteta et al. (2009a) used an online regional model, CATT-BRAMS, to investigate the sensitivity of tropical tracer transport to the convective parameterisation, and Arteta et al. (2009b) evaluated the effect of resolution on the simulated tracer distributions, showing that the higher resolution versions of their model produce more convective transport which reaches higher altitudes. Various studies (Wild and Prather, 2006; Rind et al., 2007; Deng et al., 2004) have shown that increases in horizontal and vertical resolution improve the skill of the model in predicting tracer transport by convection.

Thus far, however, there has been no concerted effort to assess the performance of short-lived tracer transport schemes across a range of global and mesoscale models. In this pair of papers we attempt to do exactly that, using a number of models which participated in the SCOUT-O3 project. These include chemical transport models, coupled chemistry-climate models or global circulation models and a mesoscale model. The resolutions, boundary layer mixing schemes and convective transport parameter-

Modelling tropical tracer transport

C. R. Hoyle et al.

[Title Page](#)[Abstract](#)[Introduction](#)[Conclusions](#)[References](#)[Tables](#)[Figures](#)[◀](#)[▶](#)[◀](#)[▶](#)[Back](#)[Close](#)[Full Screen / Esc](#)[Printer-friendly Version](#)[Interactive Discussion](#)

isations differ among the models, as does the method used to calculate the vertical winds, even when the same meteorological data is used (for the offline models). All these factors contribute to the differences in the tracer profiles the models produce. Some of the model versions which participated differed in one main aspect (see Section 2), allowing the attribution of the difference in transport to that aspect of the model configuration.

In the first paper (Russo, 2010) (hereafter R_2010), we present a comparison of the models' meteorological parameters with satellite-based measurements. In this second paper we compare the results of model tracer transport. This task is hampered by the lack of an observational quantity which can be considered as "truth": uncertainties in emissions and in chemical degradation schemes limit the degree to which any discrepancies can be ascribed to the transport schemes. Therefore, the core of our comparison is based on idealised tracers which are prescribed in the same way for all models. These reveal model-model differences but do not in themselves indicate which model's transport scheme is better. To shed light on the latter issue, a semi-realistic tracer (idealised CO) is used and compared to measurements. Since the primary source of CO in the troposphere is at the ground, it is a good tracer of upward vertical transport.

In Sect. 2 of this paper, the models which took part and their set-ups for the comparison are described. The idealised tracers and their rationale are explained in Sect. 3. The results of the comparisons are described in Sect. 4, focusing on their concentration profiles in the Tropics (4.1), the strength and spatial distribution of tropical convection (4.2), and a comparison of the idealised CO with measurements (4.4). The results are discussed in Sect. 5, as are the lessons from this first comparison of model descriptions of tracer transport in strongly convective regions.

2 Models

A total of 14 models, or model versions, participated in this inter-comparison: 7 global off-line chemical transport model (CTM) simulations, 4 global general circulation mod-

els, or coupled chemistry-climate models (GCMs, CCMs) and 3 numerical weather prediction (NWP) models. An initial series of modelling experiments were run, Round 1 (R1), and based on the results of these, the tracers were refined and a second set of experiments was carried out Round 2(R2). A summary of the configuration of these runs is provided in Table 1. The CTM, and nudged CCM model simulations were run for the year 2005, the un-nudged CCMs used boundary conditions representative of this time period. The NWP model WRF was run for February, August and November 2005, and CATT-BRAMS was run for the Maritime Continent area for November 2005. The models are described below.

2.1 TOMCAT CTM

TOMCAT is a 3-dimensional CTM with a variable horizontal and vertical resolution (Chipperfield, 2006). The model is forced using 6-hourly ECMWF analyses for vorticity, divergence, humidity and temperature. The vorticity and divergence fields provide the large-scale horizontal winds and vertical winds are diagnosed from the analysed divergence. Sub-grid scale transport is parameterised in the model using information from the large-scale analyses.

The convection scheme implemented in TOMCAT is identical to that described by Tiedtke (1989), except mid-level convection and convective down-drafts are not included and there is no organised entrainment of environmental air above cloud base (Stockwell and Chipperfield, 1999). The scheme does include cumulus up-drafts in the vertical column entrainment of environmental air into the cloud and detrainment of cloud air to the environment. The magnitudes of these are related to horizontal convergence of moisture below cloud and the difference between cloud and environmental specific humidity at cloud base. Mass balance within the vertical column is maintained by including sub-grid subsidence of environmental air (induced by convection) within the same time step.

Two TOMCAT runs were performed. For the simulation TOMCAT.Louis the model was run at $2.8^{\circ} \times 2.8^{\circ}$ with 31 hybrid σ - p levels from the surface to 10hPa. This run

Modelling tropical tracer transport

C. R. Hoyle et al.

Title Page

Abstract

Introduction

Conclusions

References

Tables

Figures



Back

Close

Full Screen / Esc

Printer-friendly Version

Interactive Discussion



used the boundary layer mixing scheme of Louis (1979).

TOMCAT_R2 is based on TOMCAT_Louis except that the boundary layer mixing scheme of Holtlag and Boville (1993) was used. Further investigation of the impact of different treatments of convection with the TOMCAT CTM is given in Feng et al. (2010)

2.2 KASIMA CTM

KASIMA is a global CTM, with a lower boundary at a pressure altitude of 4 km. The transport is calculated on a spherical grid with a T21 resolution (approximately $5.6^\circ \times 5.6^\circ$). Advection is calculated using the two-step flux-corrected scheme described by Zalesak (1979). Meteorological data from ECMWF operational analyses is used to drive the model, and the vertical wind is derived from the divergence of the horizontal winds. There is no convective transport, and no boundary layer mixing scheme.

2.3 UMCAM CCM

UMCAM is an Eulerian CCM based on the Met Office Unified Model (UM) version 4.5. The horizontal resolution is 2.5° latitude \times 3.75° longitude, with 19 vertical layers between the surface and 4.6 hPa. Convection is parameterised using the penetrative mass flux scheme of Gregory and Rowntree (1990), and the boundary layer is mixed using a MOSES-1 Non-local K scheme with entrainment (UKMO surface exchange scheme version 1). Sea surface temperatures and sea ice distribution are prescribed from the BADC dataset for 2005.

2.4 UKCA CCM

UKCA is an Eulerian GCM based on the “new dynamics” version of the Met Office UM (Davies et al., 2005). This model is non-hydrostatic and vertical velocity is calculated as a diagnostic variable on hybrid σ -height coordinates. Not using the hydrostatic approximation allows runs at very high resolution. To increase stability the model uses

Modelling tropical tracer transport

C. R. Hoyle et al.

Title Page

Abstract

Introduction

Conclusions

References

Tables

Figures

◀

▶

◀

▶

Back

Close

Full Screen / Esc

Printer-friendly Version

Interactive Discussion



a two time-level, semi-Lagrangian advection (Priestley, 1993) and semi-implicit time stepping.

The convective parameterisation scheme is based on Gregory and Rowntree (1990), and both shallow and deep convection are included. Cloud base closure for shallow convection is based on Grant (2001), and parameterised entrainment and detrainment rates for shallow convection are obtained from Grant and Brown (1999). For deep convection, the thermodynamic closure is based on the reduction of CAPE to zero (CAPE closure approach) based on Fritsch and Chappell (1980). The boundary layer parameterisation is based on Lock et al. (2000). It also includes an explicit parameterisation of entrainment at the boundary-layer top.

Three UKCA runs were performed. Run UMUKCA-UCAM (R1) is a free running version of the UKCA at the usual climate horizontal resolution of N48 (ca. $2.5^{\circ} \times 3.8^{\circ}$) and 38 levels from 0 to 39 km.

The nudged model (UMUKCA-UCAM_nud) was run at N48 resolution with 38 levels from 0 to 39 km. The nudged model uses ECMWF operational analyses available every 6 h. This data is interpolated onto the model time-steps and levels. The model temperature and horizontal winds are constrained to this data using the technique of Newtonian relaxation.

UM-UCAM_highres is a higher resolution run of the free-running UKCA model (N216, $0.83^{\circ} \times 0.56^{\circ}$) with 38 levels from 0 to 39 km. The model is initialised using UKMO assimilated initial conditions and is constrained by sea surface temperatures and sea ice derived from the GISST 2.0 climatology (Parker et al., 1995).

2.5 UMSLIMCAT CCM

UMSLIMCAT is a coupled chemistry-climate model based on the extended middle atmosphere version of UM version 4.5. Like UMCAM the horizontal resolution is 2.5° latitude \times 3.75° longitude but the model has 64 vertical levels between the surface and 0.01 hPa. Advection is calculated with the Quintic-Mono scheme (Gregory and West, 2002), and convection with the penetrative mass flux scheme (Gregory and

Modelling tropical tracer transport

C. R. Hoyle et al.

Title Page

Abstract

Introduction

Conclusions

References

Tables

Figures

◀

▶

◀

▶

Back

Close

Full Screen / Esc

Printer-friendly Version

Interactive Discussion



Rowntree, 1990). There is no mixing of tracers in the boundary layer.

2.6 Oslo CTM2

The Oslo CTM2 is a global CTM, run on 40 vertical levels between the surface and 2 hPa (hybrid σ - p coordinates) for these experiments. The mass centre of the upper model layer is at 10 hPa. The horizontal resolution used here is T42 (approx $2.8^\circ \times 2.8^\circ$). The model uses winds from the ECMWF Integrated Forecast System (IFS) model, with the vertical wind being calculated from the divergence of the horizontal fields. The meteorological input data were generated by running the IFS model at ECMWF in a series of forecasts, started from the analysed fields every 24 h (at 12:00 UTC). Each forecast was run for 36 h, allowing for 12 h of spin-up. Linking together all the forecasts results in a continuous record of input data. Data are sampled every 3 h. The forecasts were run with the cycle 29 version of the IFS model, with a spectral resolution of T319L40, which is truncated to T42 for the simulations in this study.

As well as providing large-scale winds, the IFS forecasts provide archived convective mass fluxes. The convective transport of tracers is then parameterised as an “elevator system”. Starting from the bottom of a model column, the difference in upward mass flux between the top and bottom of a model grid box determines whether entrainment or detrainment to or from the grid box takes place. If there is no difference between the fluxes through the top and bottom of the box, the up-draft simply passes through without any entrainment or detrainment of tracers. The maximum height of convection is determined by the lowest level where either precipitation flux is zero, or upward mass flux is zero. Full mixing of entrained air into the up-draft core is assumed. Turbulent mixing in the boundary layer is treated according to the Holtslag K-profile scheme Holtslag et al. (1990).

Modelling tropical tracer transport

C. R. Hoyle et al.

Title Page

Abstract

Introduction

Conclusions

References

Tables

Figures

◀

▶

◀

▶

Back

Close

Full Screen / Esc

Printer-friendly Version

Interactive Discussion



2.7 FRSGC/UCI CTM

FRSGC/UCI is a global CTM with a similar configuration to that of the Oslo CTM2. The model was run at T42 resolution for these studies, with 37 vertical layers from the surface to 2 hPa (hybrid σ - p coordinates). The mass centre of the upper model layer is at 10 hPa. The meteorological forcing data is the same as that used by the Oslo CTM2, except that the lowest 5 layers of the 40-layer output are combined into two layers. Convection is parameterised with an elevator approach based on net convective mass fluxes up through the atmospheric column, with additional treatment of explicitly defined entrainment/detrainment fluxes where these are non-zero.

2.8 pTOMCAT CTM

pTOMCAT is a global CTM originally derived from TOMCAT. It still uses the same horizontal and vertical coordinates, the same advection and convection schemes and is forced using the same ECMWF analysis files. pTOMCAT has a horizontal resolution of $2.8^\circ \times 2.8^\circ$ and 31 hybrid σ - p levels from the surface to 10 hPa. This run used the boundary layer mixing scheme of of Holtslag and Boville (1993), and is therefore very similar to run TOMCAT_R2.

In pTOMCAT-tropical, the original implementation of the convective scheme used in p-TOMCAT has been updated to increase convective transport to the mid and upper troposphere (Barret et al., 2010). The entrainment rate is set to be half the value suggested by Tiedtke (1989). This means there will be less stable ambient air entrained into the cloud and thus positive buoyancy in the cloud is retained to higher altitudes. This change offsets the problem in off-line models of diagnosing convection with analyses that have already been convectively adjusted. Other changes include using ISCCP satellite cloud data Rossow et al. (1996) to specify the fraction of saturated water vapour in each surface model grid and putting detrainment at the cloud top layer rather than in each layer between cloud top and bottom to allow a maximum lift for tracers from the boundary layer. The deep convective precipitation is set to be from

Modelling tropical tracer transport

C. R. Hoyle et al.

Title Page

Abstract

Introduction

Conclusions

References

Tables

Figures

◀

▶

◀

▶

Back

Close

Full Screen / Esc

Printer-friendly Version

Interactive Discussion



each layer's newly formed condensed liquid water.

2.9 CATT-BRAMS Regional Model

CATT-BRAMS is a regional tracer and aerosol transport model, which calculates its own meteorological data within the model domain. Deep and shallow convection are parameterised following the formulation of Grell and Dévényi (2002), as described in Arteta et al. (2009a). This scheme uses a multi-closure and multi-parameter ensemble approach with typically 144 sub-grid members. An ensemble of entrainment/detrainment profiles and/or down-draft parameters is used to determine the vertical redistribution of tracers. Turbulent mixing in the boundary layer is treated according to the level 2.5 scheme of Mellor and Yamada (1982), which employs a prognostic turbulent kinetic energy. The horizontal resolution used is 60 km×60 km (0.5°×0.5°). The simulation uses 39 vertical levels from surface to 40 km. Initial conditions are from ECMWF analyses. The model is nudged at the lateral and top boundaries with ECMWF 6-hourly analyses. Sea surface temperatures are from satellite-derived weekly analyses.

2.10 WRF NWP

WRF version 3.1.1 is a NWP model, run on 38 layers from the surface to 5 hPa using a terrain-following hydrostatic-pressure vertical coordinate system. The horizontal resolution is N96 (1.875°longitude by 1.25°latitude) and the time step is 600 s. The model uses the advective transport scheme described by Wicker and Skamarock (2002). The initial state at the surface and throughout the model atmosphere is derived from the ECMWF analyses at a spectral resolution of T511 (horizontal resolution of about 0.5°). The WRF model physics does not predict sea ice, SST, vegetation fraction, and albedo. These fields are updated in time every 6 h during the model simulation. The deep layer soil temperature is updated every 6 h as well. Sub-grid scale effects of convective and shallow clouds were parameterised by the Betts-Miller-Janjic (BMJ) cumulus scheme (Janjic, 1994, 2000). The non-resolved convective transport of tracers is parameterised

Modelling tropical tracer transport

C. R. Hoyle et al.

Title Page

Abstract

Introduction

Conclusions

References

Tables

Figures

◀

▶

◀

▶

Back

Close

Full Screen / Esc

Printer-friendly Version

Interactive Discussion



using an elevator approach based on the convective mass flux through the atmospheric column (Grell and Dévényi, 2002, as in CATT BRAMS). The mass flux is calculated using precipitation rates and cloud properties. The entrainment/detrainment profile and downdraft parameters are used to determine the vertical redistribution of tracers. Tracers are not chemically active. The surface and boundary layers are represented using the quasinormal scale elimination (QNSE) parameterisation scheme (Sukoriansky et al., 2005).

3 Methodology

3.1 Tracers

The idealised tracers which were used in the R1 and R2 modelling experiments are listed in Table 2. The definition of the tracers, and the information that they provided is as follows:

- *T20* This tracer had a lifetime of 20 days. The initial concentration was 1 pptv at the surface, and zero elsewhere. Throughout the model run the surface concentration was held constant, in the rest of the atmosphere the only loss process for the tracer was decay according to equation 1, where t is the time step and τ is the tracer lifetime. This tracer, having a lifetime similar to that of bromoform CHBr_3 , can be used to assess the differences in short-lived halogen species reaching the TTL and lowermost stratosphere between different models.

$$C = C_0 e^{-t/\tau} \quad (1)$$

- *T6h* The lifetime of this tracer was 6 h. It was initialised at the beginning of the model run with a zero mixing ratio everywhere in the atmosphere, except between the surface and 500 m, where the mass mixing ratio was set to 1 ppbm. The only loss process was decay according to equation 1. Being so short-lived, the T6h

Title Page

Abstract

Introduction

Conclusions

References

Tables

Figures

◀

▶

◀

▶

Back

Close

Full Screen / Esc

Printer-friendly Version

Interactive Discussion



**Modelling tropical
tracer transport**

C. R. Hoyle et al.

Title Page

Abstract

Introduction

Conclusions

References

Tables

Figures

◀

▶

◀

▶

Back

Close

Full Screen / Esc

Printer-friendly Version

Interactive Discussion



tracer could be used to investigate differences in the timing of rapid transport events between the surface and the upper troposphere, such as convection. The T6h tracer was also suitable for comparisons with the limited area models, as the short lifetime reduced the influence of transport from outside the model domain. Additionally, T6h required shorter spin-up times for the computationally expensive regional models.

- *CO* The idealised *CO* tracer was initialised from MOPITT data (Deeter et al., 2007) between the surface and 700 hPa. Everywhere else in the atmosphere the initial mixing ratio was zero. Loss of the tracer occurred only via reaction with a prescribed, constant mean OH field with a concentration of 0.5×10^6 molec cm^{-3} . This value is up to a factor of two lower than recent estimates of the global mean OH concentration (e.g. Wang et al., 2008), however it should be noted again that the objective was to create a highly simplified tracer which would behave with some similarity to *CO* in the atmosphere. Secondary sources of *CO* from the oxidation of hydrocarbons are also ignored, and the use of a single value for the OH concentration does not take into account latitudinal or seasonal changes in solar radiation (OH concentrations are much higher during the day than the night, and are higher in the tropics than at mid and polar latitudes). The reaction rate was pressure-dependent, given by $k = 1.5 \times 10^{-13} * (1 + 0.6P_{\text{atm}})$ (Sander et al., 2003), where P_{atm} is pressure (in atmospheres), and k has units of $\text{cm}^3 \text{ molec}^{-1} \text{ s}^{-1}$. The *CO* tracer allows a qualitative validation of modelled transport via comparisons with measured *CO* distributions.

4 Results

In this section, the fields of the modelled tracers are compared between the models as well as with observational data. The models have rather different resolutions, and even when the spacing of the grid points is similar, the actual positions often differ. For

the comparisons in Sect. 4.1, the data from each model has therefore been linearly interpolated in the necessary spatial and temporal dimensions. By interpolating to a more finely resolved grid than the best model resolution, the smoothing out of peaks or minima was avoided. For global plots, such as in Sect. 4.2, the monthly mean model data was linearly interpolated to the same grid as the Oslo CTM2, in order to compare identical pressure levels. Several of the models did not run all of the experiments, therefore some models are not included in each of the plots shown below.

4.1 Tropical concentration profiles

We start our analysis with the T6h tracer; this tracer's mixing ratio decreases by half in ~4 h and goes to zero after ~24 h. Because of its extremely short lifetime this tracer can only experience fast transport processes and its vertical profile will be therefore mainly affected by convective transport. To analyse the convective transport in the different models using T6h (and T20 in the next section), we focus on 3 geographical regions, namely South America, West Africa and the Maritime Continent (hereafter abbreviated as SA, WA and MC), which have been chosen to provide examples of different types of land and island deep convection. The convective transport in each of these regions is analysed for one month chosen so that the region exhibits a strong convective activity (see R_2010 for further discussion on the choice of the regions and the respective months). The monthly mean vertical profiles of T6h are shown in Fig. 1, averaged over SA in February, WA in August and MC in November. Additionally we show for comparison the annual mean tracer profile averaged over the whole tropical region (note that only a subset of the models have archived the necessary information for this plot). In R_2010, we performed a detailed comparison of modelled and observed cloud top height distributions to investigate differences in the strength of the convection and the ability of convective parameterisations to reproduce the observed vertical distributions of clouds. Here we investigate how the same convective parameterisations differ in the vertical transport of tracers. In particular we focus on the height of the mean convective outflow and the tracer's peak concentrations at the outflow relative to the surface

Modelling tropical tracer transport

C. R. Hoyle et al.

Title Page

Abstract

Introduction

Conclusions

References

Tables

Figures

◀

▶

◀

▶

Back

Close

Full Screen / Esc

Printer-friendly Version

Interactive Discussion



Modelling tropical tracer transport

C. R. Hoyle et al.

Title Page

Abstract

Introduction

Conclusions

References

Tables

Figures

◀

▶

◀

▶

Back

Close

Full Screen / Esc

Printer-friendly Version

Interactive Discussion



concentration. If one compares the same model in different regions, the changes in the height of the tracer's main convective outflow should be determined by changes in the vertical extent of the convection, while the changes in tracer's peak concentration at the outflow should follow changes in the number of convective events reaching that height. However, differences between models are not always directly attributable to such changes. In fact, the way models parameterise venting of the boundary layer, and entrainment-detrainment rates in the convective plume, can have a larger impact on the tracer distribution than the vertical extent or frequency of the convection. For example some models use convective schemes which release the tracer at the top of the convection while others distribute the tracer throughout the convective column. Therefore one should keep in mind that differences between models vertical profiles of T6h are not always directly attributable to differences in the vertical extent of the convection or the number of convective events. For this reason, the meteorological analysis of convective properties in R_2010 will help to attribute differences in the model's convective transport.

We first analyse the height of the mean convective outflow and how it varies between models and between different geographical locations compared to the tropical mean. For the tropical region, 20° N–20° S, we can distinguish between two sets of models, those with a mean convective outflow at a height of ~190 hPa (~12.5 km) and those with a lower convective outflow at ~300 hPa (~9 km). These two model categories are also clearly marked for SA, with outflow heights at 190–200 hPa and 300 hPa respectively. For the MC region the outflow heights of the first set of models are further split between ~150 hPa (~14 km) for CATT-BRAMS and pTOMCAT_tropical, and 190–200 hPa for most other models, while TOMCAT and pTOMCAT outflow heights remain around 300 hPa. For the WA region, differences in the height of the convective outflow are smaller, with values of ~180–200 hPa for most models and 250 hPa (~10.5 km) for TOMCAT and pTOMCAT. The lower outflow heights displayed by TOMCAT and pTOMCAT can be explained by the cloud top height analysis in R_2010: with the exception of the WA region, these two models show a consistently smaller percentage of clouds

reaching above 10 km compared to observations and other models. This indicates that the vertical extent of tropical convection, and the associated fast vertical transport, might be underestimated in these models.

Most of the models are either forced or nudged by the ECMWF winds (the only exceptions in Fig. 1 being WRF, CATT-BRAMS and UM-UCAM_highres. The span of results between the different models shows that the short-lived tracer transport depends more on the details of the convective parameterisation than on the forcing data, or the model resolution.

Indeed, modifying the convective parameterisation scheme in pTOMCAT (pTOMCAT_tropical, shown as the dashed line in Fig. 1) produces cloud top heights which are in better agreement with observations (see also R_2010); the tracer's convective outflow for this modified version is also significantly higher, and very similar to the high resolution CATT-BRAMS model, which uses its own dynamics as opposed to ECMWF forcing.

In general, the relative heights of the convective outflow for the different models do not change significantly with geographical location, with the exception of TOMCAT and pTOMCAT which have significantly higher outflow heights for WA compared to all other regions. CATT-BRAMS and pTOMCAT_tropical have the highest outflow heights (150 hPa, ~14 km for the MC region), and although the cloud top height analysis in R_2010 does not point to them as having the highest percentage of high clouds, this apparent discrepancy can be explained by the fact that both these models have convective detrainment at the top of the cloud rather than throughout the column. FRSGC/UCI, Oslo CTM2, WRF, UMUKCA-UCAM_nud and UM-UCAM_highres have fairly similar convective outflow heights for all regions (in the range 170–200 hPa (~13–12 km), with FRSGC/UCI, Oslo CTM2 and WRF being slightly higher for some regions compared to the two UCAM models. The cloud top analysis in R_2010 shows that the cloud top distributions are highest for FRSGC/UCI, Oslo CTM2, and UMUKCA-UCAM_nud, and slightly lower for WRF and UM-UCAM_highres. In this case, the inconsistency between the high cloud tops produced by UMUKCA-UCAM_nud and the relatively lower convec-

Modelling tropical tracer transport

C. R. Hoyle et al.

Title Page

Abstract

Introduction

Conclusions

References

Tables

Figures

◀

▶

◀

▶

Back

Close

Full Screen / Esc

Printer-friendly Version

Interactive Discussion



tive outflow height can be attributed to the fact that the cloud fraction within the large model gridbox ($3.7^{\circ} \times 2.5^{\circ}$) starts decreasing with height above ~ 13 km.

We now analyse the tracer mixing ratio at the convective outflow and how it varies between models and between different geographical locations compared to the tropical mean. Generally FRSGC/UCI, Oslo CTM2 and WRF have the largest mixing ratios at the level of convective outflow, while TOMCAT and/or UМУKCA-UCAM_nud have the lowest. The other models are generally in between. The profiles from UM-UCAM_highres and UМУKCA-UCAM_nud are similar in all regions except WA, where the high resolution version of the model produces both a larger, and a higher altitude peak in tracer concentrations than the nudged model. Over SA, the nudged model has a much more pronounced mid-tropospheric minimum than UM-UCAM_highres. The very low monthly-mean tracer mixing ratio produced by UМУKCA-UCAM_nud for WA results from an anomalously low number of convective events for this region compared to other regions; this is thought to be due to poor representation of surface properties (such as surface albedo and soil moisture). Comparing the tracer mixing ratios at the outflow height between the different regions shows that for the Tropics, the tracer mixing ratios at the convective outflow height vary within the range 0.9–2.5% of the mixing ratio imposed at the surface. These values are generally smaller compared to mixing ratios at the convective outflow for the three different domains, which show mixing ratios in the range 1.4–5%, 0.5–3.5%, and 1–7% for SA, WA, and MC respectively (note that for WA we have ignored the anomalously low value associated to UМУKCA-UCAM_nud). The generally larger mixing ratios for these regions suggests that for most models under investigation, convective transport from the surface to the convective outflow height level is more efficient in these three regions at the selected times compared to the annual average convective transport in the whole tropical region. One exception is West Africa: for this region TOMCAT, pTOMCAT, pTOMCAT_tropical and UМУKCA-UCAM_nud have smaller mixing ratios at the convective outflow than they have for the Tropics.

While convection lifts the T6h tracer typically only to its convective outflow height,

Modelling tropical tracer transport

C. R. Hoyle et al.

Title Page

Abstract

Introduction

Conclusions

References

Tables

Figures

◀

▶

◀

▶

Back

Close

Full Screen / Esc

Printer-friendly Version

Interactive Discussion



differences between models in the outflow height and in the tracer mixing ratio at this level will also have an impact on the amount of surface species which are subsequently transported upward from the TTL to the lower stratosphere.

The data in Fig. 1 can also be viewed as a time series, as shown in Fig. 2. Due to the short lifetime of T6h, a marked diurnal cycle is expected in the upper tropospheric mixing ratios, and indeed, there is some periodicity in the T6h mixing ratios for all of the models, resulting from a daily cycle of maxima and minima in rates of transport from the surface to higher levels in the troposphere. Again here, differences in both the altitude of maximum outflow, as well as the strength of the vertical transport are obvious and cannot always be attributed to differences in the model used to generate the meteorological forcing data. A surprising difference between the models, considering that many of them use meteorological forcing data from the same source, is that the timing of the changes in the intensity of the vertical transport is not identical.

The FRSGC/UCI and Oslo CTM2 produce similar time series, differing from those of pTOMCAT and TOMCAT (R2) mainly by mixing ratio, and altitude. At the very beginning of the time series, both FRSGCUCI and Oslo CTM2 show moderate transport to higher levels, while pTOMCAT and TOMCAT (R2) show very little vertical transport in this period, apart from this the timing in the results is similar.

UMUKCA-UCAM_nud shows greater transport to about 200hPa at days 305–308, a feature which is not seen in the TOMCAT (R2) or pTOMCAT plots. The lower convective activity around day 320 is seen in all of the models, however it starts 1–2 days earlier for TOMCAT (R2), pTOMCAT and UМУKCA-UCAM_nud than the other models. The free-running models produce results similar to the general features of the convective activity seen in the forced models. The timing of the enhanced concentrations in the upper troposphere differs slightly between UМУKCA-UCAM_nud and UM-UCAM_highres, for example around day 315.

The magnitude of the daily changes in transport intensity differ greatly between the models. CATT-BRAMS has the strongest daily cycle in convective activity, with T6h mixing ratios almost completely decaying in between the convective peaks, while the other

Modelling tropical tracer transport

C. R. Hoyle et al.

Title Page

Abstract

Introduction

Conclusions

References

Tables

Figures

◀

▶

◀

▶

Back

Close

Full Screen / Esc

Printer-friendly Version

Interactive Discussion



models have far less variability in the upper troposphere. UМУKCA-UCAM_nud produces fairly constant enhanced mixing ratios at about 700hPa, while in CATT-BRAMS, Oslo CTM2 and FRSGC/UCI the lower tropospheric peak mixing ratios are much more variable.

5 The differences in tropospheric transport are carried on into the stratosphere, where the spread between the models further increases, as shown in Fig. 3. While the maximum difference between the November mean mixing ratio over the Maritime Continent of two models (UMSLIMCAT and FRSGC/UCI) was about a factor of three at around 100 hPa, by 70 hPa it is already more than an order of magnitude, and continues to increase with increasing altitude. There are two processes contributing to the divergence of the modelled mixing ratios, firstly the altitude at which the slow up-welling of the lower stratosphere begins, and secondly, different rates of the stratospheric up-welling between the models. For example, while the upper tropospheric peak in mixing ratios from UMCAM is lower than that of FRSGC/UCI over WA and SA, higher in the stratosphere UMCAM has the larger mixing ratios, due to faster vertical transport within the lowermost stratosphere. On the other hand, in the tropical mean panel, FRSGC/UCI has greater mixing ratios in the upper troposphere than pTOMCAT, and the difference in mixing ratios continues to increase with altitude, due to a faster lower stratospheric up-welling in FRSGC/UCI than in pTOMCAT. However, the use of analysed divergence fields to calculate vertical transport in the TOMCAT/pTOMCAT model is known to over-estimate the rate of vertical tracer transport, for example in compared to the use of heating rates (Monge-Sanz et al., 2007).

15 In Fig. 3, the lowest tracer concentrations in the lower troposphere, except in West Africa, are those of TOMCAT_Louis. The difference between TOMCAT (R2) and TOMCAT_Louis is the boundary layer mixing scheme employed in the model, the Louis scheme restricting the amount of tracer mixing into the lower troposphere far more than the scheme used in TOMCAT (R2). This leads to significantly smaller mixing ratios for TOMCAT_Louis than TOMCAT (R2) up to about 100 hPa. The boundary layer mixing scheme therefore, has the potential to influence tracer mixing ratios throughout

Modelling tropical tracer transport

C. R. Hoyle et al.

Title Page

Abstract

Introduction

Conclusions

References

Tables

Figures

◀

▶

◀

▶

Back

Close

Full Screen / Esc

Printer-friendly Version

Interactive Discussion



the troposphere. The profile for KASIMA starts at 600 hPa, as this is the lower boundary of the model. Due to the lack of a convective transport parameterisation, the profile of KASIMA shows no pronounced upper tropospheric peak, and has smaller mixing ratios than the profiles of the other models in the upper most troposphere and lower-most stratosphere. The profiles from UМУKCA-UCAM_nud and UМУKCA-UCAM (R1) look very similar except over the MC, where the nudged version produces higher tracer mixing ratios in the middle troposphere, more in line with the results of the other models. Over WA, the situation is reversed, with the nudged version showing lower mixing ratios than all the other models between about 800 hPa and 400 hPa.

4.2 Location of convection

The geographical location of convection is important as it determines the mixing ratios of water and the chemical species transported to the upper troposphere and the lower stratosphere. The idea of a “stratospheric fountain”, with air preferentially entering the stratosphere over the western tropical Pacific and the Maritime Continent, was put forward by Newell and Gould-Stewart (1981). Subsequently Holton and Gettelman (2001) pointed out that the observed stratospheric water vapour mixing ratios could also be explained if air passed more or less horizontally through a cold area (“cold trap”) in the upper troposphere, but did not necessarily enter the stratosphere at that location. Transport from the tropical boundary layer to the tropical tropopause layer and the stratosphere during January 2001 was investigated by Levine et al. (2007), who found that two thirds of the transport from the planetary boundary layer to the TTL occurs vertically over the Indian Ocean, Indonesia and the western Pacific. On the other hand, Ricaud et al. (2007) found that convective transport of trace gases into the lower most stratosphere mainly takes place above land convective regions, particularly Africa.

The annual mean enhancement in T20 mixing ratio at approximately 200 hPa is shown in Fig. 4. This was calculated by dividing the annual mean T20 mixing ratio at each grid point by the annual, global mean mixing ratio on the 200 hPa level. The

Modelling tropical tracer transport

C. R. Hoyle et al.

Title Page

Abstract

Introduction

Conclusions

References

Tables

Figures

◀

▶

◀

▶

Back

Close

Full Screen / Esc

Printer-friendly Version

Interactive Discussion



highest T20 mixing ratios are seen in the tropics, indicating the greatest amount of vertical transport to this level takes place there, as expected. The width of the band of high convective activity does not vary greatly between the models, and all models show the greatest vertical transport taking place over the western Pacific and Indian Ocean.

5 Most of the models also show transport being slightly enhanced over South America and Africa. At 90 hPa (Figure 5), the picture is similar, with most models indicating that the vast majority of the upward transport is taking place over the western Pacific and Indian Ocean, with very little contribution from other areas. FRSGC/UCI, Oslo CTM2, TOMCAT and pTOMCAT also show smaller contributions over South America and western Africa. No data was available at the 90 hPa level for UМУKCA-UCAM_nud.

10 The seasonal cycle of the T20 mixing ratios at 90 hPa in the three areas SA, WA, MC as well as a tropical mean are shown in Fig. 6. The 90 hPa level was chosen as it is located well into the TTL and is above the level of zero radiative heating. Tracers reaching this level will likely be transported into the lower stratosphere. Over SA, most of the models show a seasonal variation with minima from about July to September and larger mixing ratios from about January to March. A similar pattern is seen over the MC with low values from about June to September and larger values in November and December. The mixing ratios over the MC are also generally larger than in the other areas, which leads to the general cycle over the MC being similar to that seen in the tropical mean. In contrast to the other models, UMSLIMCAT shows a peak in T20 concentration in August–September over the MC. Over WA, few of the models show significant variation throughout the year, exceptions are UMCAM and UМУKCA-UCAM (R1), which both show larger mixing ratios towards the middle of the year. In the tropical average, mixing ratios are generally smaller from about July to October, and larger from November to May. UMSLIMCAT has a peak in mixing ratio in September, corresponding to the similar peak in over the MC, and UМУKCA-UCAM (R1) has elevated mixing ratios in July to August, which is related to the similar feature seen over WA. The seasonal cycles in T20 mixing ratio shown in Fig. 6 should relate to the precipitation rates shown in Fig. 3 of R_2010. Over South America, all models show a marked

Modelling tropical tracer transport

C. R. Hoyle et al.

Title Page

Abstract

Introduction

Conclusions

References

Tables

Figures

◀

▶

◀

▶

Back

Close

Full Screen / Esc

Printer-friendly Version

Interactive Discussion



seasonal cycle in precipitation rates, which is reflected in the T20 mixing ratios shown in Fig. 6. There is no direct relationship between amplitude of seasonal changes in the precipitation and amplitude of the seasonal changes in T20 for the different models, e.g. Oslo CTM2 and FRSGC/UCI have the highest amplitude changes in T20 mixing ratios and approximately the lowest amplitude change in precipitation rate. The situation is similar over the MC.

Over WA, there is also a seasonal cycle in precipitation rates, however, as described above, there is no pronounced seasonal cycle in T20 mixing ratios at 90 hPa for most of the models. At 200 hPa (not shown), most of the models show a seasonal cycle over WA which correlates with the changes in precipitation throughout the year. Therefore, according to these models, the vertical transport from the surface to 90hPa is strongly linked to convection for the MC and SA but not for WA.

4.3 Impact of location of rapid transport on TTL composition

The dependence of upper tropospheric tracer mixing ratios on the location of rapid vertical transport in the models can be assessed using the idealised tracers. Firstly, the monthly mean T20 mixing ratios are used to determine the grid boxes where the transport time between the surface and 153 hPa are the shortest (the highest T20 mixing ratios, similar to the areas in each panel of Fig. 5 where the mixing ratios are the highest). Then, for each month, the tropical mean (20° N–20° S) CO mixing ratio at 153 hPa is plotted as a function of the surface mixing ratio of CO averaged over the points where the transport time was determined to be the shortest. The plot of 153 hPa tropical mean CO mixing ratio vs. CO surface mixing ratio in the active vertical transport regions is shown in the upper panel of Fig. 7. For most of the models, there is a clear correlation between the two values, with correlation coefficients (R) as high as 0.90, as shown in Table 3. In contrast, when the 153 hPa tropical mean CO is plotted against the mean of the CO surface mixing ratios in the less active vertical transport regions (lower panel), the correlation is much smaller. The gradient of a linear fit to the points plotted for each model was also calculated (M in Table 3), and the much larger

Modelling tropical tracer transport

C. R. Hoyle et al.

Title Page

Abstract

Introduction

Conclusions

References

Tables

Figures

◀

▶

◀

▶

Back

Close

Full Screen / Esc

Printer-friendly Version

Interactive Discussion



gradients in the regions with faster transport (upper panel of Fig. 7) show that in the most active transport regions, a smaller change in CO can lead to a greater effect in the upper troposphere. The fact that in the lower panel the gradients are much smaller, show that it is the surface mixing ratio in the areas with the most rapid transport that control the UT/LS CO mixing ratios. There is however some contribution from the less convectively active areas, as for a few points, the upper tropospheric CO mixing ratios are larger than the surface mixing ratios in the convectively active areas. It is also interesting to note that the surface CO mixing ratios are generally smaller in the areas with faster transport to the upper troposphere. As can be seen in Fig. 5, these areas are often over the ocean, where the air is less polluted.

The lower boundary condition for CO was a monthly varying, prescribed mixing ratio between the surface and 700 hPa, therefore using a CO mixing ratio from slightly higher in the boundary layer would not have affected the results. The correlation between upper tropospheric tracer mixing ratio and location of convection show that it is important for the modelling of the composition of the tropical tropopause region that the areas of rapid vertical transport in the models are correctly located.

4.4 Comparison with measurements

The idealised CO tracer used in the models has a uniform removal rate and no additional sources, therefore it cannot be expected to exactly reproduce the observed tracer fields on a particular day. It can still be used however, to evaluate general features of the model transport, such as the representation of seasonal cycles or the strength and altitude of the transport of lower tropospheric air to the upper troposphere. Because of its relatively long photochemical lifetime, the distribution of CO is determined to a large extent by transport processes, although there is also a significant atmospheric source, due to the oxidation of hydrocarbons and methane (e.g. Shindell et al., 2006).

During the SCOUT-O3 measurement campaign carried out in the area of Darwin, Australia, in November and December 2005, the concentration of CO was measured with the COLD (Cryogenically Operated Laser Diode) instrument on board the Geo-

Modelling tropical tracer transport

C. R. Hoyle et al.

Title Page

Abstract

Introduction

Conclusions

References

Tables

Figures

◀

▶

◀

▶

Back

Close

Full Screen / Esc

Printer-friendly Version

Interactive Discussion



physica research aircraft. The COLD instrument is a mid-infrared tunable diode laser airborne spectrometer for in-situ measurement of trace gases. A liquid nitrogen cooled lead-salt diode laser is used in combination with an astigmatic Herriott multi-pass cell (providing an optical path of 36 m) to detect the absorption signal of the molecules under analysis. A direct absorption detection technique, which does not need in-flight calibration, is employed in conjunction with fast sweep integration. For CO measurements, an in-flight sensitivity of few ppbv is achieved, with a time resolution of 4 s, a precision of 1% and an accuracy in the range 6–9%, mainly due to the accuracy of the molecular database (Viciani et al., 2008).

The modelled idealised CO fields were interpolated to the measurement times and locations along the Geophysica flight track, and a comparison with the measured data is plotted in Fig. 8. One of the focuses of the SCOUT-O3 measurement campaign in Darwin was to measure air that had been affected by the strong convective systems (“Hector”) which form over the Tiwi islands (Brunner et al., 2009). On the 16th of November, air in the outflow of a Hector was sampled. On the 23rd of November the quiescent TTL was sampled, and on the 25th of November only weak convection was observed. On 30th of November, relatively strong convection influenced the sampled air masses.

In general, all the models produce idealised CO values which are similar to the measured values. On the 16th, UMUKCA-UCAM_nud underestimates the measured CO mixing ratio in the lower -mid troposphere, while at about 350 hPa, pTOMCAT overestimates the mixing ratios. Higher in the atmosphere, around 100 hPa, most of the models match better with the convectively perturbed CO values than the background values, with UMUKCA-UCAM_nud still returning the lowest mixing ratios, which are within the range of the measurements. On the 30th of November, again the models capture the UT/LS CO as well as the slope of the decay in mixing ratios as altitude continues to increase. Lower down, however, there are substantial over-estimations of the measured values by all models.

On the less convectively active days, such as the 23rd of November, the models

Modelling tropical tracer transport

C. R. Hoyle et al.

Title Page

Abstract

Introduction

Conclusions

References

Tables

Figures

◀

▶

◀

▶

Back

Close

Full Screen / Esc

Printer-friendly Version

Interactive Discussion



**Modelling tropical
tracer transport**

C. R. Hoyle et al.

Title Page

Abstract

Introduction

Conclusions

References

Tables

Figures

◀

▶

◀

▶

Back

Close

Full Screen / Esc

Printer-friendly Version

Interactive Discussion



capture the lower troposphere mixing ratios, however they all overestimate the values measured between about 150 hPa and 60 hPa, while on the 25th, the models generally reproduce the lower to mid tropospheric CO mixing ratios but, except for UMUKCA-UCAM_nud, overestimate the CO above 100 hPa. Some of the offset of the models towards higher CO values may be due to the idealised CO tracer having a longer lifetime than CO in the atmosphere. In general, the models all seem to have a vertical transport that corresponds more to convectively influenced profiles.

The agreement of the models with the measurements is encouraging, but it should be kept in mind that the differences between the models decrease as the lifetime of the tracer increases, and with a lifetime of around 3 months, CO is considerably longer lived than many of the halogen species with lifetimes of the order of days or weeks, such as bromoform (with a lifetime of about 30 days), although dibromomethane is actually much longer lived (with a lifetime of over 6 months, (Hossaini et al., 2010)).

Measurements of CO made by the Tropospheric Emission Spectrometer (TES) instrument, averaged over an area bounded by 4.2°, 20.9°, 131 hPa and 110 hPa for the northern and southern hemispheres are plotted along with modelled CO in Fig. 9. TES is an infrared Fourier transform spectrometer which was launched on-board NASA Aura satellite in 2004 (Beer et al., 2001). TES is the first satellite instrument to provide vertical information on tropospheric ozone whilst simultaneously measuring CO on a global basis. The data used in this study comes from the TES Global Survey operating mode in which TES makes nadir observations with a 5.3×8.3 km footprint providing near global coverage approximately every 16 days. TES ozone and CO profiles are provided on 67 vertical levels from the surface to 0.1 hPa and have been extensively validated against in-situ observations (Nassar et al., 2008; Osterman et al., 2008; Richards et al., 2008; Luo et al., 2007; Lopez et al., 2008).

In order to correctly compare TES and model profiles one must account for the limited vertical resolution and the effects of a priori information inherent in the retrieved TES profiles. This is achieved through the application of the TES observation operator to the model profile. The observation operator consists of the averaging kernels and

the a priori profile used in the retrieval (Rodgers and Connor, 2003). The application of the TES operator to a comparison profile is described in detail in Worden et al. (2007). For this study the unique TES observation operator for each TES profile was applied to each model profile before averaging the resulting profiles for monthly mean comparisons.

All the models follow the seasonal cycle seen in the TES data, with CO values being larger in October-December than during the rest of the year. The spread between the modelled CO mixing ratios is larger in the Northern Hemisphere than in the Southern Hemisphere, with values in July ranging from around 75ppbv (pTOMCAT) to 90ppbv (FRSGC/UCI), and from 100ppbv (pTOMCAT) to 115ppbv (FRSGC/UCI) in November. The smallest differences from the TES CO mixing ratios in the northern hemisphere are seen for pTOMCAT, UMUKCA-UCAM_nud and the Oslo CTM2. In the southern hemisphere, the TES mixing ratios are underestimated slightly by most of the models between July and October, while in November and December TOMCAT (R2) and FRSGC/UCI overestimate the TES values. The highest CO mixing ratios in the southern hemisphere are measured by TES in October. All the models except pTOMCAT, however, have the peak in November.

5 Discussion

For the offline models, i.e. those which use a pre-calculated set of meteorological forcing data, the short lived tracer distribution is influenced to a large extent by the transport parameterisations in the model. Specifically, the choice of boundary layer mixing scheme has a large influence on the tropospheric tracer profile, as less dispersive schemes limit the flux of a tracer emitted at ground level into the free troposphere. When comparing the profiles from TOMCAT_Louis and TOMCAT_R2 in Fig. 3, the influence of the boundary layer mixing scheme on a short lived tracer can be seen throughout the tracer profile, up to at least 100 hPa. For the offline models pTOMCAT and pTOMCAT-tropical, the only difference is the way in which the convective trans-

Modelling tropical tracer transport

C. R. Hoyle et al.

Title Page

Abstract

Introduction

Conclusions

References

Tables

Figures

◀

▶

◀

▶

Back

Close

Full Screen / Esc

Printer-friendly Version

Interactive Discussion



Modelling tropical tracer transport

C. R. Hoyle et al.

Title Page

Abstract

Introduction

Conclusions

References

Tables

Figures

◀

▶

◀

▶

Back

Close

Full Screen / Esc

Printer-friendly Version

Interactive Discussion



port is calculated. The large differences in their T6h and T20 profiles shown in Figs. 1 and 3 again illustrate the significant influence of the convective parameterisation. The only model which does not contain a convective transport parameterisation, KASIMA, also produced a tracer profile with smaller concentrations than the other models up to 100 hPa. Over the middle portion of the tropical mean profile around 150 hPa-400 hPa, KASIMA and TOMCAT_Louis produced very similar T20 concentrations, smaller than the remaining models, further under-scoring the importance of the choice of boundary layer mixing scheme, and the use of an accurate convective transport parameterisation, when studying tropospheric tracer transport. The nudged version of UKCA (UMUKCA-UCAM_nud) shows significantly lower mixing ratios for the T6h tracer over parts of the profile for SA and WA, than is the case for the high resolution free running version (UM-UCAM_highres). Better agreement with other models is achieved with (UM-UCAM_highres). Despite the lack of an explicit boundary layer mixing scheme, UMSLIMCAT did not have a tropospheric tracer profile which was significantly different from that of the other models.

For extremely short-lived species (with lifetimes of the order of hours to days), the influence of the models' transport parameterisations are even more obvious. Despite the use of ECMWF meteorological data to drive the models, there is around 100 hPa of difference in the altitude at which detrainment results in peak tracer concentrations, between several of the models. All aspects of the tracer distribution, i.e. the profile shape, the concentrations and the timing of transport events differ between several of the models which use the ECMWF data. Clearly, despite the use of forcing data from the same source, the transport parameterisations play a substantial role in determining the tracer distribution.

All of the models reproduced the observed seasonal cycles in mean upper tropospheric CO well, in comparison with the TES measurements, suggesting that the differences in model transport remain relatively constant throughout the year. Differences in the geographical location of the most rapid vertical transport were also examined, and it was found that the mean upper tropospheric CO mixing ratio in the tropics at

153hPa is correlated with the CO mixing ratio at the surface below the area of most rapid vertical transport in the model. Models with vertical transport taking place over areas with greater concentrations of anthropogenic species may therefore have a more polluted upper troposphere in the tropics.

5 For tracers with a lifetime of the order of a month, a priority should be for the model to reproduce the observed altitude at which tracer detrainment occurs. For shorter lived tracers, the intensity of the transport also becomes increasingly important. The timing of the transport events is probably of lesser importance for average tracer mixing ratios, unless there is a systematic difference between the models, as in the long term
10 the amount of tracer transported into the upper troposphere will not strongly depend on the timing of the events. On the other hand, if the timing of the transport events is linked to the stability of the boundary layer in the different models, this may create a systematic difference in the amount of tracer transported upwards. For the composition of air entering the lowermost stratosphere, the combination of convective detrainment height and vertical advection rate in the UT/LS is important, models with a low convective detrainment altitude may still have larger mixing ratios of CO, for example, in the lowermost stratosphere, because of a more rapid advection above the convective outflow. The impact of differences in the strength of convection and detrainment altitude of convection between the models depends on the lifetime of the tracer and the
20 altitude of interest. Throughout the troposphere, the modelled profiles of all tracers differed among the models, however, for altitudes of 100 hPa and higher, the idealised CO tracer profiles from all models were similar. For the shorter-lived tracers T20 and T6h, large differences in concentration at these altitudes were found, with the differences between models being greater for the very short-lived tracer T6h than T20.

25 During the course of this study, it became clear that there is a need for measurements of tracers with which model transport can be validated, independently of model chemistry. Such a tracer should have relatively well defined emissions at the surface, be insoluble, and have a short lifetime via a loss process which is independent of other atmospheric species and of altitude. The only tracer which really fits this profile is

Modelling tropical tracer transport

C. R. Hoyle et al.

Title Page

Abstract

Introduction

Conclusions

References

Tables

Figures

◀

▶

◀

▶

Back

Close

Full Screen / Esc

Printer-friendly Version

Interactive Discussion



radon. Although radon has been used in several studies in the past (e.g. Jacob et al., 1997), there is no extensive data set suitable for model evaluation. Despite the difficulties in measuring radon in the atmosphere (Kritz et al., 1998), the feasibility of large scale measurements of radon throughout the atmosphere should be considered in the future – such a dataset would improve the existing possibilities for model validation enormously.

Acknowledgements. This work was supported with funding from the EU project SCOUT-O3. CRH was partly funded by SNSF grant number 200021_120175/1. NRPH thanks NERC for their Advanced Research Fellowship. NADR is funded via NERC NCEO. The CATT-BRAMS work was supported by the program LEFE/INSU in France (projects UTLS-tropicale and Tropopause 2009) and was performed using HPC resources of CINES under the allocation 2008- c2008012536 and 2009 -c2009015036 made by GENCI (Grand Equipement National de Calcul Intensif).

References

- Arteta, J., Marécal, V., and Rivière, E. D.: Regional modelling of tracer transport by tropical convection – Part 1: Sensitivity to convection parameterization, *Atmos. Chem. Phys.*, 9, 7081–7100, doi:10.5194/acp-9-7081-2009, 2009a. 20359, 20366
- Arteta, J., Marécal, V., and Rivière, E. D.: Regional modelling of tracer transport by tropical convection - Part 2: Sensitivity to model resolutions, *Atmos. Chem. Phys.*, 9, 7101–7114, doi:10.5194/acp-9-7101-2009, 2009b. 20359
- Barret, B., Williams, J. E., Bouarar, I., Yang, X., Josse, B., Law, K., Pham, M., Le Flochmoën, E., Liousse, C., Peuch, V. H., Carver, G. D., Pyle, J. A., Sauvage, B., van Velthoven, P., Schlager, H., Mari, C., and Cammas, J.-P.: Impact of West African Monsoon convective transport and lightning NO_x production upon the upper tropospheric composition: a multi-model study, *Atmos. Chem. Phys. Discuss*, 2245–2302, doi:10.5194/acpd-10-2245-2010, doi:10.5194/acp-10-5719-2010, 2010. 20365, 20393
- Beer, R., Glavich, T., and Rider, D.: Tropospheric emission spectrometer for the Earth Observing System's Aura Satellite, *Appl. Opt.*, 40, 2356–2367, 2001. 20380

Modelling tropical tracer transport

C. R. Hoyle et al.

Title Page

Abstract

Introduction

Conclusions

References

Tables

Figures

◀

▶

◀

▶

Back

Close

Full Screen / Esc

Printer-friendly Version

Interactive Discussion



**Modelling tropical
tracer transport**

C. R. Hoyle et al.

Title Page

Abstract

Introduction

Conclusions

References

Tables

Figures

◀

▶

◀

▶

Back

Close

Full Screen / Esc

Printer-friendly Version

Interactive Discussion



- Berntsen, T., Fuglestvedt, J., Myhre, G., Stordal, F., and Berglen, T.: Abatement of greenhouse gases: Does location matter?, *Climatic Change*, 74, 377–411, doi:10.1007/s10584-006-0433-4, 2006. 20393
- 5 Brunner, D., Siegmund, P., May, P. T., Chappel, L., Schiller, C., Mueller, R., Peter, T., Fueglistaler, S., MacKenzie, A. R., Fix, A., Schlager, H., Allen, G., Fjaeraa, A. M., Streibel, M., and Harris, N. R. P.: The SCOUT-O3 Darwin Aircraft Campaign: rationale and meteorology, *Atmos. Chem. Phys.*, 9, 93–117, doi:10.5194/acp-9-93-2009, 2009. 20379
- Chipperfield, M. P.: New version of the TOMCAT/SLIMCAT off-line chemical transport model: Intercomparison of stratospheric tracer experiments, *Q. J. Roy. Meteorol. Soc.*, 132, 1179–1203, doi:10.1256/qj.05.51, 2006. 20361, 20393
- 10 Corti, T., Luo, B. P., Peter, T., Vömel, H., and Fu, Q.: Mean radiative energy balance and vertical mass fluxes in the equatorial upper troposphere and lower stratosphere, *Geophys. Res. Lett.*, 32, doi:10.1029/2004GL021889, 2005. 20359
- Davies, T., Cullen, M., Malcolm, A., Mawson, M., Staniforth, A., White, A., and Wood, N.: A new dynamical core for the Met Office's global and regional modelling of the atmosphere, *Q. J. Roy. Meteorol. Soc.*, 131, 1759–1782, doi:10.1256/qj.04.101, 2005. 20362
- 15 Deeter, M. N., Edwards, D. P., Gille, J. C., and Drummond, J. R.: Sensitivity of MOPITT observations to carbon monoxide in the lower troposphere, *J. Geophys. Res.*, 112, doi:10.1029/2007JD008929, 2007. 20368
- 20 Deng, A., Seaman, N., Hunter, G., and Stauffer, D.: Evaluation of interregional transport using the MM5-SCIPUFF system, *J. Appl. Meteorol.*, 43, 1864–1886, 2004. 20359
- Feng, W., Chipperfield, M. P., Dorf, M., Pfeilsticker, K., and Ricaud, P.: Mid-latitude ozone changes: studies with a 3-D CTM forced by ERA-40 analyses, *Atmos. Chem. Phys.*, 7, 2357–2369, doi:10.5194/acp-7-2357-2007, 2007. 20358
- 25 Feng, W., Chipperfield, M. P., Dhomse, S., Monge-Sanz, B., and Yang, X.: Evaluation of cloud convection and tracer transport in a three-dimensional chemical transport model, in preparation, *Atmos. Chem. Phys.*, 2010. 20362
- Folkins, I., Loewenstein, M., Podolske, J., Oltmans, S., and Proffitt, M.: A barrier to vertical mixing at 14 km in the tropics: Evidence from ozonesondes and aircraft measurements, *J. Geophys. Res.*, 104, 22095–22102, 1999. 20359
- 30 Folkins, I., Oltmans, S., and Thompson, A.: Tropical convective outflow and near surface equivalent potential temperatures, *Geophys. Res. Lett.*, 27, 2549–2552, 2000. 20359
- Folkins, I., Bernath, P., Boone, C., Donner, L. J., Eldering, A., Lesins, G., Martin, R. V., Sinnhu-

**Modelling tropical
tracer transport**

C. R. Hoyle et al.

Title Page

Abstract

Introduction

Conclusions

References

Tables

Figures

◀

▶

◀

▶

Back

Close

Full Screen / Esc

Printer-friendly Version

Interactive Discussion



ber, B. M., and Walker, K.: Testing convective parameterizations with tropical measurements of HNO_3 , CO , H_2O , and O_3^- : Implications for the water vapor budget, *J. Geophys. Res.*, 111, doi:10.1029/2006JD007325, 2006. 20359

5 Freitas, S. R., Longo, K. M., Dias, M. A. F. S., Chatfield, R., Dias, P. S., Artaxo, P., Andreae, M. O., Grell, G., Rodrigues, L. F., Fazenda, A., and Panetta, J.: The Coupled Aerosol and Tracer Transport model to the Brazilian developments on the Regional Atmospheric Modeling System (CATT-BRAMS) – Part 1: Model description and evaluation, *Atmos. Chem. Phys.*, 9, 2843–2861, doi:10.5194/acp-9-2843-2009, 2009. 20393

10 Fritsch, J. M. and Chappell, C. F.: Numerical prediction of convectively driven mesoscale pressure systems.1. Convective parameterization, *J. Atmos. Sci.*, 37, 1722–1733, 1980. 20363
Fueglistaler, S., Dessler, A. E., Dunkerton, T. J., Folkins, I., Fu, Q., and Mote, P. W.: Tropical Tropopause Layer, *Rev. Geophys.*, 47, doi:10.1029/2008RG000267, 2009. 20358, 20359

Grant, A.: Cloud-base fluxes in the cumulus-capped boundary layer, *Q. J. Roy. Meteorol. Soc.*, 127, 407–421, 2001. 20363

15 Grant, A. and Brown, A.: A similarity hypothesis for shallow-cumulus transports, *Q. J. Roy. Meteorol. Soc.*, 125, 1913–1936, 1999. 20363

Gregory, A. and West, V.: The sensitivity of a model's stratospheric tape recorder to the choice of advection scheme, *Q. J. Roy. Meteorol. Soc.*, 128, 1827–1846, 2002. 20363, 20393

20 Gregory, D. and Rowntree, P. R.: A mass flux convection scheme with representation of cloud ensemble characteristics and stability-dependent closure, *Mon. Weather Rev.*, 118, 1483–1506, 1990. 20362, 20363

Grell, G. and Dévényi, D.: A generalized approach to parameterizing convection combining ensemble and data assimilation techniques, *Geophys. Res. Lett.*, doi:10.1029/2002GL015311, 2002. 20366, 20367

25 Hartmann, D. L. and Larson, K.: An important constraint on tropical cloud - climate feedback, *Geophys. Res. Lett.*, 29, doi:10.1029/2002GL015835, 2002. 20359

Holton, J. and Gettelman, A.: Horizontal transport and the dehydration of the stratosphere, *Geophys. Res. Lett.*, 28, 2799–2802, 2001. 20375

Holtstlag, A., Debruin, E., and Pan, H.: A high-resolution air-mass transformation model for short-range weather forecasting, *Mon. Weather Rev.*, 118, 1561–1575, 1990. 20364, 20393

30 Holtstlag, A. A. M. and Boville, B. A.: Local versus nonlocal boundary-layer diffusion in a global climate model, *J. Climate*, 6, 1825–1842, 1993. 20362, 20365, 20393

Hossaini, R., Chipperfield, M. P., Monge-Sanz, B. M., Richards, N. A. D., Atlas, E., and Blake,

Modelling tropical tracer transport

C. R. Hoyle et al.

[Title Page](#)[Abstract](#)[Introduction](#)[Conclusions](#)[References](#)[Tables](#)[Figures](#)[◀](#)[▶](#)[◀](#)[▶](#)[Back](#)[Close](#)[Full Screen / Esc](#)[Printer-friendly Version](#)[Interactive Discussion](#)

D. R.: Bromoform and dibromomethane in the tropics: a 3-D model study of chemistry and transport, *Atmos. Chem. Phys.*, 10, 719–735, doi:10.5194/acp-10-719-2010, 2010. 20358, 20380

Jacob, D., Prather, M., Rasch, P., Shia, R., Balkanski, Y., Beagley, S., Bergmann, D., Blackshear, W., Brown, M., Chiba, M., Chipperfield, M., deGrandpre, J., Dignon, J., Feichter, J., Genthon, C., Grose, W., Kasibhatla, P., Kohler, I., Kritz, M., Law, K., Penner, J., Ramonet, M., Reeves, C., Rotman, D., Stockwell, D., VanVelthoven, P., Verver, G., Wild, O., Yang, H., and Zimmermann, P.: Evaluation and intercomparison of global atmospheric transport models using Rn-222 and other short-lived tracers, *J. Geophys. Res.*, 102, 5953–5970, 1997. 20384

Janjic, Z.: The Step-Mountain ETA Coordinate model - further developments of the convection, viscous sublayer, and turbulence closure schemes, *Mon. Weather Rev.*, 122, 927–945, 1994. 20366

Janjic, Z.: Comments on “Development and evaluation of a convection scheme for use in climate models”, *J. Atmos. Sci.*, 57, 3686, 2000. 20366

Kouker, W., Offermann, D., Kull, V., Reddmann, T., Ruhnke, R., and Franzen, A.: Streamers observed by the CRISTA experiment and simulated in the KASIMA model, *J. Geophys. Res.*, 104, 16405–16418, 1999. 20393

Kritz, M., Rosner, S., and Stockwell, D.: Validation of an off-line three-dimensional chemical transport model using observed radon profiles – 1. Observations, *J. Geophys. Res.*, 103, 8425–8432, 1998. 20384

Kupper, C., Thuburn, J., Craig, G. C., and Birner, T.: Mass and water transport into the tropical stratosphere: A cloud-resolving simulation, *J. Geophys. Res.*, 109, doi:10.1029/2004JD004541, 2004. 20359

Laube, J. C., Engel, A., Boenisch, H., Moebius, T., Worton, D. R., Sturges, W. T., Grunow, K., and Schmidt, U.: Contribution of very short-lived organic substances to stratospheric chlorine and bromine in the tropics - a case study, *Atmos. Chem. Phys.*, 8, 7325–7334, doi:10.5194/acp-8-7325-2008, 2008. 20358

Law, K. S. and Sturges, W. T.: Halogenated very short-lived substances, in: WMO Scientific Assessment of Ozone Depletion 2006: Global ozone research and monitoring project, Rep. 50, World Meteorol. Org., Geneva, 2007. 20358

Leonard, B. P., Lock, A. P., and Macvean, M. K.: The nirvana scheme applied to one-dimensional advection, *Int. J. Num. Meth. Heat Fluid Flow*, 5, 341–377, 1995. 20393

Levine, J. G., Braesicke, P., Harris, N. R. P., Savage, N. H., and Pyle, J. A.: Pathways

and timescales for troposphere-to-stratosphere transport via the tropical tropopause layer and their relevance for very short lived substances, *J. Geophys. Res.*, 112, doi:10.1029/2005JD006940, 2007. 20375

5 Liang, Q., Stolarski, R. S., Kawa, S. R., Nielsen, J. E., Douglass, A. R., Rodriguez, J. M., Blake, D. R., Atlas, E. L., and Ott, L. E.: Finding the missing stratospheric Br_y: a global modeling study of CHBr₃ and CH₂Br₂, *Atmos. Chem. Phys.*, 10, 2269–2286, doi:10.5194/acp-10-2269-2010, 2010. 20358

10 Lock, A., Brown, A., Bush, M., Martin, G., and Smith, R.: A new boundary layer mixing scheme. Part I: Scheme description and single-column model tests, *Mon. Weather Rev.*, 128, 3187–3199, 2000. 20363, 20393

Lopez, J. P., Luo, M., Christensen, L. E., Loewenstein, M., Jost, H., Webster, C. R., and Osterman, G.: TES carbon monoxide validation during two AVE campaigns using the Argus and ALIAS instruments on NASA's WB-57F, *J. Geophys. Res.*, 113, doi:10.1029/2007JD008811, 2008. 20380

15 Louis, J. F.: Parametric model of vertical eddy fluxes in the atmosphere, *Bound.-Layer Meteorol.*, 17, 187–202, 1979. 20362, 20393

Luo, M., Rinsland, C., Fisher, B., Sachse, G., Diskin, G., Logan, J., Worden, H., Kulawik, S., Osterman, G., Eldering, A., Herman, R., and Shephard, M.: TES carbon monoxide validation with DACOM aircraft measurements during INTEX-B 2006, *J. Geophys. Res.*, 112, doi:10.1029/2007JD008803, 2007. 20380

20 Mellor, G. and Yamada, T.: Development of a turbulence closure-model for geophysical fluid problems, *Rev. Geophys.*, 20, 851–875, 1982. 20366, 20393

Monge-Sanz, B. M., Chipperfield, M. P., Simmons, A. J., and Uppala, S. M.: Mean age of air and transport in a CTM: Comparison of different ECMWF analyses, *Geophys. Res. Lett.*, 34, doi:10.1029/2006GL028515, 2007. 20374

25 Morgenstern, O., Braesicke, P., O'Connor, F. M., Bushell, A. C., Johnson, C. E., Osprey, S. M., and Pyle, J. A.: Evaluation of the new UKCA climate-composition model. Part 1: The stratosphere, *Geosci. Model Dev.*, 43–57, 2009. 20393

30 Nassar, R., Logan, J. A., Worden, H. M., Megretskaia, I. A., Bowman, K. W., Osterman, G. B., Thompson, A. M., Tarasick, D. W., Austin, S., Claude, H., Dubey, M. K., Hocking, W. K., Johnson, B. J., Joseph, E., Merrill, J., Morris, G. A., Newchurch, M., Oltmans, S. J., Posny, F., Schmidlin, F. J., Voemel, H., Whiteman, D. N., and Witte, J. C.: Validation of Tropospheric Emission Spectrometer (TES) nadir ozone profiles using ozonesonde measurements, *J.*

Modelling tropical tracer transport

C. R. Hoyle et al.

Title Page

Abstract

Introduction

Conclusions

References

Tables

Figures

◀

▶

◀

▶

Back

Close

Full Screen / Esc

Printer-friendly Version

Interactive Discussion



- Geophys. Res., 113, D15S17, doi:10.1029/2007JD008819, 2008. 20380
- Newell, R. and Gould-Stewart, S.: A Stratospheric Fountain, *J. Atmos. Sci.*, 38, 2789–2796, 1981. 20375
- O'Connor, F. M., Carver, G. D., Savag, N. H., Pyle, J. A., Methven, J., Arnold, S. R., Dewey, K., and Kent, J.: Comparison and visualisation of high-resolution transport modelling with aircraft measurements, *Atmos. Sci. Lett.*, 6, 164–170, 2005. 20393
- Osterman, G. B., Kulawik, S. S., Worden, H. M., Richards, N. A. D., Fisher, B. M., Eldering, A., Shephard, M. W., Froidevaux, L., Labow, G., Luo, M., Herman, R. L., Bowman, K. W., and Thompson, A. M.: Validation of Tropospheric Emission Spectrometer (TES) measurements of the total, stratospheric, and tropospheric column abundance of ozone, *J. Geophys. Res.*, 113, doi:10.1029/2007JD008801, 2008. 20380
- Park, M., Randel, W. J., Emmons, L. K., Bernath, P. F., Walker, K. A., and Boone, C. D.: Chemical isolation in the Asian monsoon anticyclone observed in Atmospheric Chemistry Experiment (ACE-FTS) data, *Atmos. Chem. Phys.*, 8, 757–764, doi:10.5194/acp-8-757-2008, 2008. 20358
- Parker, D., Jackson, M., and Horton, E.: The 1961-1990 GISS 2.2 Sea Surface Temperature and Sea Ice Climatology, Climate Research Technical Note No. 63, Hadley Centre for Climate Prediction and Research, Bracknell, UK, 1995. 20363
- Petch, J. C., Willett, M., Wong, R. Y., and Woolnough, S. J.: Modelling suppressed and active convection. Comparing a numerical weather prediction, cloud-resolving and single-column model, *Q. J. Roy. Meteorol. Soc.*, 133, 1087–1100, doi:10.1002/qj.109, 2007. 20393
- Prather, M.: Numerical advection by conservation of 2nd-order moments, *J. Geophys. Res.*, 91, 6671–6681, 1986. 20393
- Priestley, A.: A quasi-conservative version of the semi-lagrangian advection scheme, *Mon. Weather Rev.*, 121, 621–629, 1993. 20363, 20393
- Ricaud, P., Barret, B., Attie, J. L., Motte, E., Le Flochmoeen, E., Teyssedre, H., Peuch, V. H., Livesey, N., Lambert, A., and Pommereau, J. P.: Impact of land convection on troposphere-stratosphere exchange in the tropics, *Atmos. Chem. Phys.*, 7, 5639–5657, doi:10.5194/acp-7-5639-2007, 2007. 20359, 20375
- Richards, N. A. D., Osterman, G. B., Browell, E. V., Hair, J. W., Avery, M., and Li, Q.: Validation of Tropospheric Emission Spectrometer ozone profiles with aircraft observations during the intercontinental chemical transport experiment-B, *J. Geophys. Res.*, 113, doi:10.1029/2007JD008815, 2008. 20380

Modelling tropical tracer transport

C. R. Hoyle et al.

Title Page

Abstract

Introduction

Conclusions

References

Tables

Figures

◀

▶

◀

▶

Back

Close

Full Screen / Esc

Printer-friendly Version

Interactive Discussion



**Modelling tropical
tracer transport**

C. R. Hoyle et al.

Title Page

Abstract

Introduction

Conclusions

References

Tables

Figures

◀

▶

◀

▶

Back

Close

Full Screen / Esc

Printer-friendly Version

Interactive Discussion



- Rind, D., Lerner, J., Jonas, J., and McLinden, C.: Effects of resolution and model physics on tracer transports in the NASA Goddard Institute for Space Studies general circulation models, *J. Geophys. Res.*, 112, D09315, doi:10.1029/2006JD007476, 2007. 20359
- Rodgers, C. D. and Connor, B. J.: Intercomparison of remote sounding instruments, *J. Geophys. Res.*, 4116, doi:10.1029/2002JD002299, 2003. 20381
- Rossow, W., Walker, A., Beuschel, D., and Roiter, M.: International Satellite Cloud Climatology Project (ISCCP) Documentation of New Cloud Datasets, Tech. Rep. WMO/TD-No. 737, World Meteorological Organization, 1996. 20365
- Russo, M.: Tropical deep convection and its impact on composition in global and mesoscale models: meteorology, in preparation, 2010. 20360
- Salawitch, R. J., Weisenstein, D. K., Kovalenko, L. J., Sioris, C. E., Wennberg, P. O., Chance, K., Ko, M. K. W., and McLinden, C. A.: Sensitivity of ozone to bromine in the lower stratosphere, *Geophys. Res. Lett.*, 32, L05811, doi:10.1029/2004GL021504, 2005. 20358
- Sander, S., Friedl, R. R., Ravishankara, A. R., Golden, D. M., Kolb, C. E., Kurylo, M. J., Huie, R. E., L., O. V., J., M. M., K., M. G., and J., F.-P. B.: Chemical Kinetics and Photochemical Data for Use in Atmospheric Studies, Tech. rep., JPL Publication 02-25, 2003. 20368
- Sherwood, S. C. and Dessler, A. E.: On the control of stratospheric humidity, *Geophys. Res. Lett.*, 27, 2513–2516, 2000. 20359
- Shindell, D. T., Faluvegi, G., Stevenson, D. S., Krol, M. C., Emmons, L. K., Lamarque, J. F., Petron, G., Dentener, F. J., Ellingsen, K., Schultz, M. G., Wild, O., Amann, M., Atherton, C. S., Bergmann, D. J., Bey, I., Butler, T., Cofala, J., Collins, W. J., Derwent, R. G., Doherty, R. M., Drevet, J., Eskes, H. J., Fiore, A. M., Gauss, M., Hauglustaine, D. A., Horowitz, L. W., Isaksen, I. S. A., Lawrence, M. G., Montanaro, V., Mueller, J. F., Pitari, G., Prather, M. J., Pyle, J. A., Rast, S., Rodriguez, J. M., Sanderson, M. G., Savage, N. H., Strahan, S. E., Sudo, K., Szopa, S., Unger, N., van Noije, T. P. C., and Zeng, G.: Multimodel simulations of carbon monoxide: Comparison with observations and projected near-future changes, *J. Geophys. Res.*, 111, doi:10.1029/2006JD007100, 2006. 20378
- Sinnhuber, B. M. and Folkens, I.: Estimating the contribution of bromoform to stratospheric bromine and its relation to dehydration in the tropical tropopause layer, *Atmos. Chem. Phys.*, 6, 4755–4761, doi:10.5194/acp-6-4755-2006, 2006. 20358
- Skamarock, W. C., Klemp, J. B., Dudhia, J., Gill, D. O., Barker, D. M., Duda, M. G., Huang, X.-Y., Wang, W., and Powers, J. G.: A description of the Advanced Research WRF Version 3, NCAR Technical Note NCAR/TN-475+STR, NCAR, NCAR Boulder, CO, USA, 2008. 20393

**Modelling tropical
tracer transport**

C. R. Hoyle et al.

Title Page

Abstract

Introduction

Conclusions

References

Tables

Figures

◀

▶

◀

▶

Back

Close

Full Screen / Esc

Printer-friendly Version

Interactive Discussion



- Stockwell, D. Z. and Chipperfield, M. P.: A tropospheric chemical-transport model: Development and validation of the model transport schemes, *Q. J. Roy. Meteorol. Soc.*, 125, 1747–1783, 1999. 20361
- Sturges, W. T., Oram, D. E., Carpenter, L. J., Penkett, S. A., and Engel, A.: Bromoform as a source of stratospheric bromine, *Geophys. Res. Lett.*, 27, 2081–2084, 2000. 20358
- Sukoriansky, S., Galperin, B., and Staroselsky, I.: A quasnormal scale elimination model of turbulent flows with stable stratification, *Phys. Fluid.*, 17, 085107, doi:10.1063/1.2009010, 2005. 20367, 20393
- Telford, P. J., Braesicke, P., Morgenstern, O., and Pyle, J. A.: Technical Note: Description and assessment of a nudged version of the new dynamics Unified Model, *Atmos. Chem. Phys.*, 8, 1701–1712, doi:10.5194/acp-8-1701-2008, 2008. 20393
- Tian, W. and Chipperfield, M.: A new coupled chemistry-climate model for the stratosphere: The importance of coupling for future O-3-climate predictions, *Q. J. Roy. Meteorol. Soc.*, 131, 281–303, doi:10.1256/qj.04.05, 2005. 20393
- Tiedtke, M.: A comprehensive mass flux scheme for cumulus parameterization in large-scale models, *Mon. Weather Rev.*, 117, 1779–1800, 1989. 20361, 20365
- Tremback, C. J., Powell, J., Cotton, W. R., and Pielke, R. A.: The forward-in-time upstream advection scheme – extension to higher orders, *Mon. Weather Rev.*, 115, 540–555, 1987. 20393
- Viciani, S., D’Amato, F., Mazzinghi, P., Castagnoli, F., Toci, G., and Werle, P.: A cryogenically operated laser diode spectrometer for airborne measurement of stratospheric trace gases, *Applied Physics B-Lasers and Optics*, B90, 581–592, doi:10.1007/s00340-007-2885-2, 2008. 20379
- Wang, J. S., McElroy, M. B., Logan, J. A., Palmer, P. I., Chameides, W. L., Wang, Y., and Megretskaia, I. A.: A quantitative assessment of uncertainties affecting estimates of global mean OH derived from methyl chloroform observations, *J. Geophys. Res.*, doi:10.1029/2007JD008496, 2008. 20368
- Wicker, L. and Skamarock, W.: Time-splitting methods for elastic models using forward time schemes, *Mon. Weather Rev.*, 130, 2088–2097, 2002. 20366
- Wild, O. and Prather, M. J.: Global tropospheric ozone modeling: Quantifying errors due to grid resolution, *J. Geophys. Res.*, 111, doi:10.1029/2005JD006605, 2006. 20359
- Wild, O., Prather, M., Akimoto, H., Sundet, J., Isaksen, I., Crawford, J., Davis, D., Avery, M., Kondo, Y., Sachse, G., and Sandholm, S.: Chemical transport model ozone simulations for

- spring 2001 over the western Pacific: Regional ozone production and its global impacts, *J. Geophys. Res.*, 109, D15S02, doi:10.1029/2003JD004041, 2004. 20393
- Worden, H. M., Logan, J. A., Worden, J. R., Beer, R., Bowman, K., Clough, S. A., Eldering, A., Fisher, B. M., Gunson, M. R., Herman, R. L., Kulawik, S. S., Lampel, M. C., Luo, M., Megretskaiia, I. A., Osterman, G. B., and Shephard, M. W.: Comparisons of Tropospheric Emission Spectrometer (TES) ozone profiles to ozonesondes: Methods and initial results, *J. Geophys. Res.*, 112, D03309, doi:10.1029/2006JD007258, 2007. 20381
- Zalesak, S.: Fully multidimensional flux-corrected transport algorithms for fluids, *J. Comput. Phys.*, 31, 335–362, 1979. 20362, 20393
- 10 Zeng, G. and Pyle, J.: Changes in tropospheric ozone between 2000 and 2100 modeled in a chemistry-climate model, *Geophys. Res. Lett.*, 30, 1392, doi:10.1029/2002GL016708, 2003. 20393

Modelling tropical tracer transport

C. R. Hoyle et al.

[Title Page](#)[Abstract](#)[Introduction](#)[Conclusions](#)[References](#)[Tables](#)[Figures](#)[I◀](#)[▶I](#)[◀](#)[▶](#)[Back](#)[Close](#)[Full Screen / Esc](#)[Printer-friendly Version](#)[Interactive Discussion](#)

Modelling tropical tracer transport

C. R. Hoyle et al.

Table 1. The models which participated in the inter-comparison.

Model	Type	Resolution	Transport	BL mix.	Circulation	Reference
Round 1						
¹ TOMCAT_Louis	CTM	2.8°×2.8°L31	Prather (1986)	Louis (1979)	ECMWF operational	Chipperfield (2006)
² KASIMA	CTM	5.6°×5.6°, 750 m	Zalesak (1979)	no BL	ECMWF operational	Kouker et al. (1999)
³ UMCAM	CCM	2.5°×3.8°L19	Leonard et al. (1995)	see text	N/A	Zeng and Pyle (2003)
⁴ UMUKCA-UCAM (R1)	CCM	2.5°×3.8°L38	semi-Lagrangian	Lock et al. (2000)	N/A	Morgenstern et al. (2009)
⁵ UMSLIMCAT	CCM	2.5°×3.8°L64	Gregory and West (2002)	no mixing	N/A	Tian and Chipperfield (2005)
Round 2						
⁶ Oslo CTM2	CTM	2.8°×2.8°L40	Prather (1986)	Holtslag et al. (1990)	ECMWF IFS cycle 29	Berntsen et al. (2006)
⁷ FRSGC/UCI	CTM	2.8°×2.8°L37	Prather (1986)	Holtslag et al. (1990)	ECMWF IFS cycle 29	Wild et al. (2004)
⁸ TOMCAT (R2)	CTM	2.8°×2.8°L31	Prather (1986)	Holtslag and Boville (1993)	ECMWF operational	Chipperfield (2006)
⁹ pTOMCAT	CTM	2.8°×2.8°L31	Prather (1986)	Holtslag and Boville (1993)	ECMWF operational	O'Connor et al. (2005)
¹⁰ pTOMCAT-tropical	CTM	2.8°×2.8°L31	Prather (1986)	Holtslag and Boville (1993)	ECMWF operational	Barret et al. (2010)
¹¹ UMUKCA-UCAM_nud	nudged GCM	2.5°×3.8°L38	Priestley (1993)	Lock et al. (2000)	Nudged with ECMWF operational	Telford et al. (2008)
¹² UM-UCAM_highres	global NWP	0.6°×0.8°L38	Priestley (1993)	Lock et al. (2000)	Initialised from UKMO	Petch et al. (2007)
¹³ CATT-BRAMS	Regional NWP	60 km×60 km L39	Tremback et al. (1987)	Mellor and Yamada (1982)	Initialised from ECMWF	Freitas et al. (2009)
¹⁴ WRF	global NWP	1.9°×1.3°L38	Skamarock et al. (2008)	Sukoriansky et al. (2005)	Initialised from ECMWF	Skamarock et al. (2008)

The models were run at the following institutions:

^{1,5,8} University of Leeds

² Karlsruhe Institute of Technology

^{3,4,9,10,11,12} University of Cambridge

⁶ University of Oslo

⁷ Lancaster University

¹³ Météo-France and CNRS and University of Orléans

¹⁴ University of Herfordshire

[Title Page](#)
[Abstract](#)
[Introduction](#)
[Conclusions](#)
[References](#)
[Tables](#)
[Figures](#)
[Back](#)
[Close](#)
[Full Screen / Esc](#)
[Printer-friendly Version](#)
[Interactive Discussion](#)


Modelling tropical tracer transport

C. R. Hoyle et al.

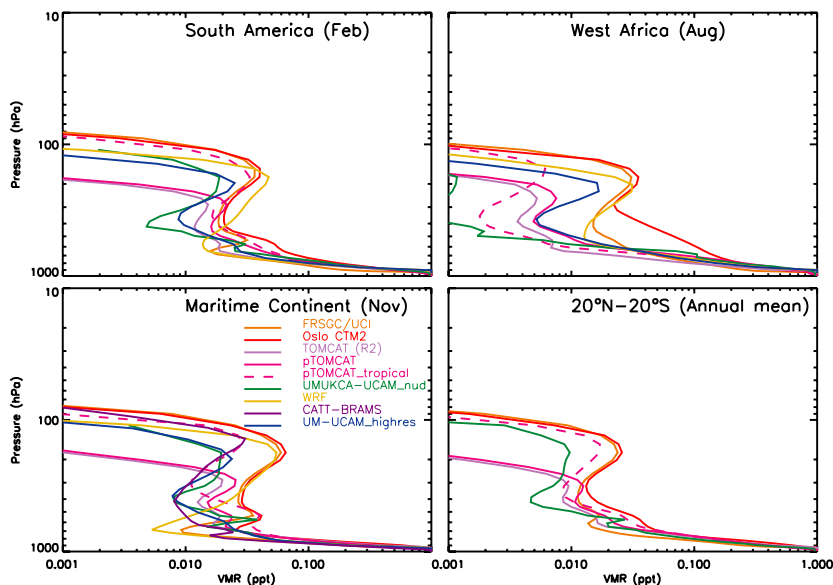


Fig. 1. The mean profile of T6h volume mixing ratios, for each model, averaged over three different areas for particular months of 2005, as well as an annual mean for the tropical region (lower right panel).

[Title Page](#)[Abstract](#)[Introduction](#)[Conclusions](#)[References](#)[Tables](#)[Figures](#)[◀](#)[▶](#)[◀](#)[▶](#)[Back](#)[Close](#)[Full Screen / Esc](#)[Printer-friendly Version](#)[Interactive Discussion](#)

Modelling tropical
tracer transport

C. R. Hoyle et al.

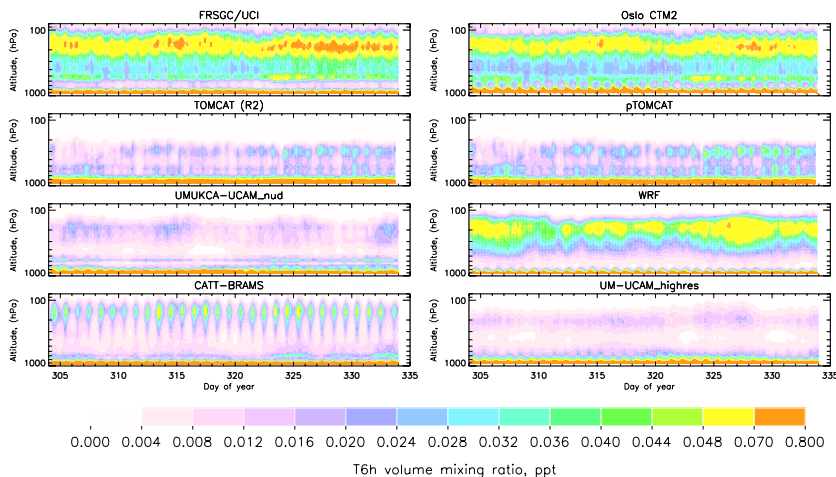


Fig. 2. Modelled profiles of mass mixing ratio as a function of time, for T6h, averaged over the Maritime Continent. The data runs from day 304 to 334, i.e. midnight on the 1st of November 2005 to midnight on the 30th of November 2005.

Title Page

Abstract

Introduction

Conclusions

References

Tables

Figures

◀

▶

◀

▶

Back

Close

Full Screen / Esc

Printer-friendly Version

Interactive Discussion



Modelling tropical tracer transport

C. R. Hoyle et al.

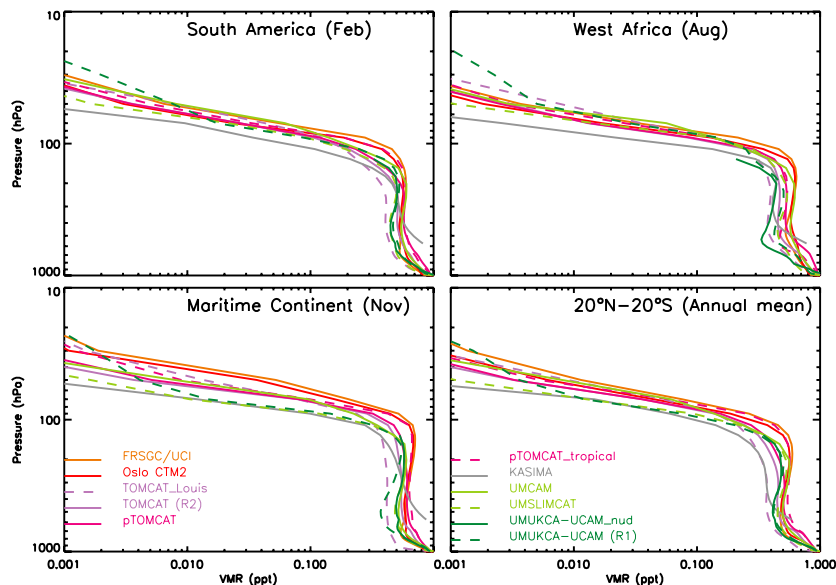


Fig. 3. The mean profile of T20 volume mixing ratios, for each model, averaged over three different areas for particular months of 2005, as well as an annual, tropical mean (lower right panel). The legend is split over the lower two plots, but refers to all four plots. No data was available for UМУKCA-UCAM_nud above 90 hPa.

Title Page

Abstract

Introduction

Conclusions

References

Tables

Figures

◀

▶

◀

▶

Back

Close

Full Screen / Esc

Printer-friendly Version

Interactive Discussion



Modelling tropical tracer transport

C. R. Hoyle et al.

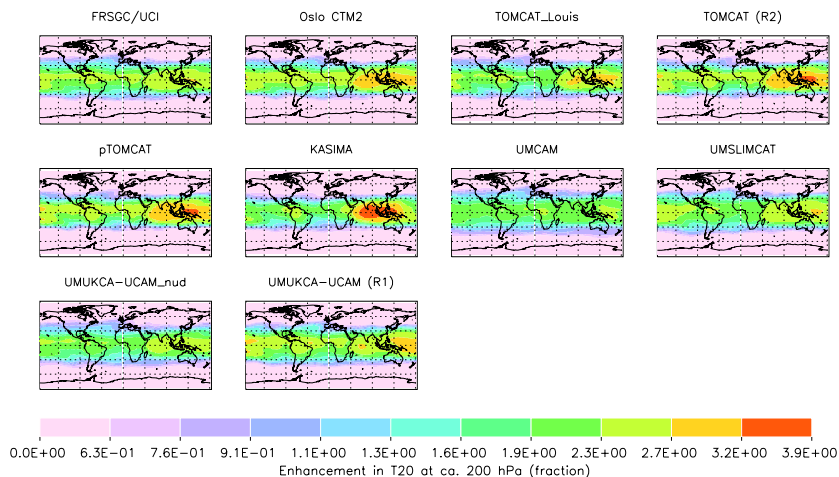


Fig. 4. The fraction enhancement of the 2005 annual mean mixing ratio of the T20 tracer, for each model, at the 200 hPa level. The enhancement was calculated by dividing the value at a particular point by the global mean at that level.

Title Page

Abstract

Introduction

Conclusions

References

Tables

Figures

◀

▶

◀

▶

Back

Close

Full Screen / Esc

Printer-friendly Version

Interactive Discussion



Modelling tropical tracer transport

C. R. Hoyle et al.

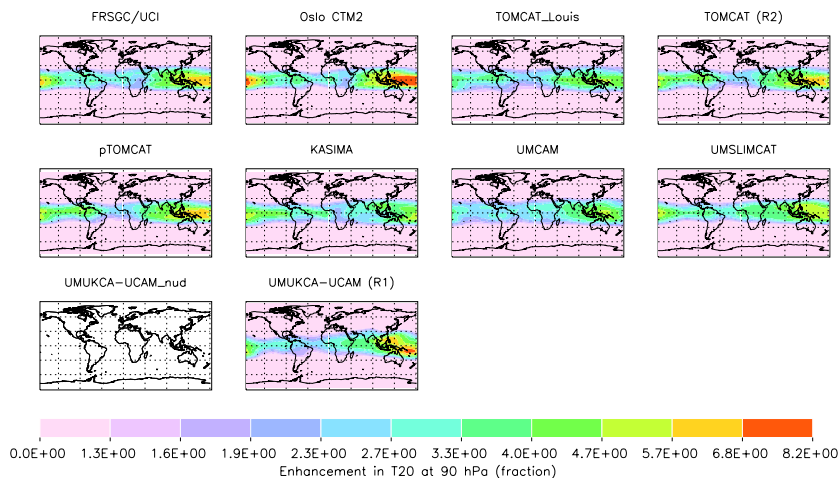


Fig. 5. The fraction enhancement of the 2005 annual mean mixing ratio of the T20 tracer, for each model at the 90 hPa level. No data was available at this level for UМУKCA-UCAM_nud. The enhancement was calculated by dividing the value at a particular point by the global mean at that level.

Title Page

Abstract Introduction

Conclusions References

Tables Figures

◀ ▶

◀ ▶

Back Close

Full Screen / Esc

Printer-friendly Version

Interactive Discussion



Modelling tropical tracer transport

C. R. Hoyle et al.

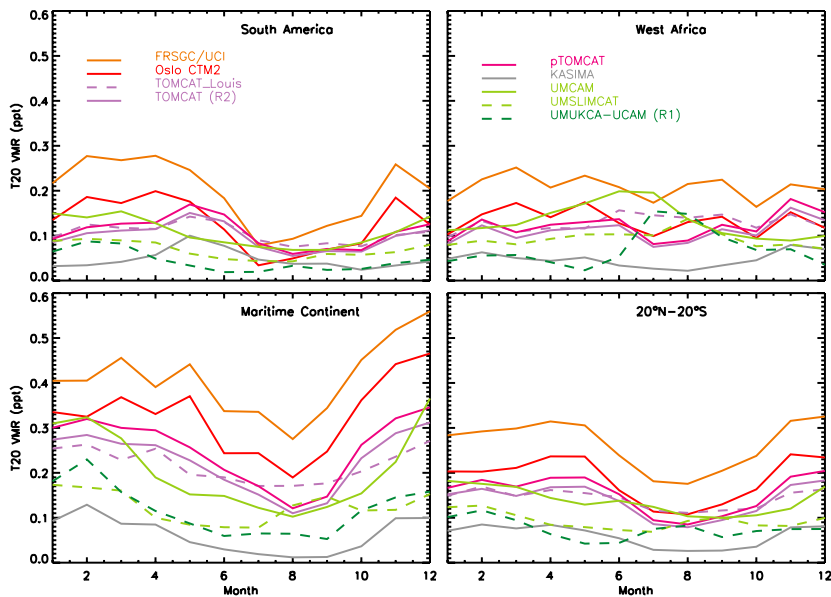


Fig. 6. The variation throughout 2005 of the T20 mixing ratio in the different models at 90 hPa over SA, WA, the MC and as a tropical mean. The legend is split over the two lower panels, but applies to all panels.

Title Page

Abstract

Introduction

Conclusions

References

Tables

Figures

◀

▶

◀

▶

Back

Close

Full Screen / Esc

Printer-friendly Version

Interactive Discussion



Modelling tropical
tracer transport

C. R. Hoyle et al.

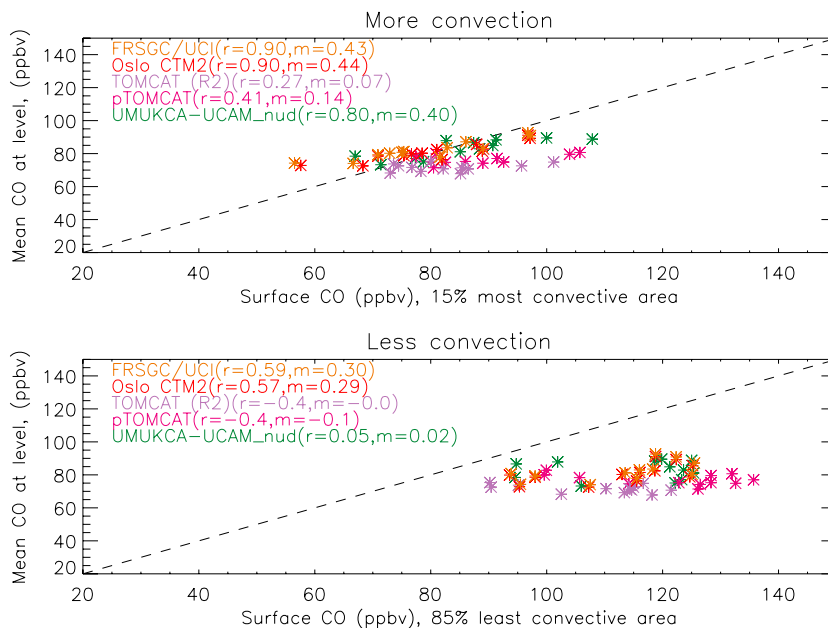


Fig. 7. The tropical mean CO mixing ratios at 153 hPa vs mean surface CO mixing ratios. Values are plotted for each model and each month (monthly means) of 2005. The surface CO mixing ratios in the upper panel were taken from the 15% of the model surface, between 20° S and 20° N, directly below the grid boxes at 153 hPa with the highest T20 mixing ratios (indicating the 15% shortest transport times from the surface to 153 hPa). The surface mixing ratios in the lower panel represent the average of the remaining 85% of the area between 20° S and 20° N. The correlation coefficients and the slopes of fit lines are given in Table 3.

Title Page

Abstract

Introduction

Conclusions

References

Tables

Figures

◀

▶

◀

▶

Back

Close

Full Screen / Esc

Printer-friendly Version

Interactive Discussion



Modelling tropical tracer transport

C. R. Hoyle et al.

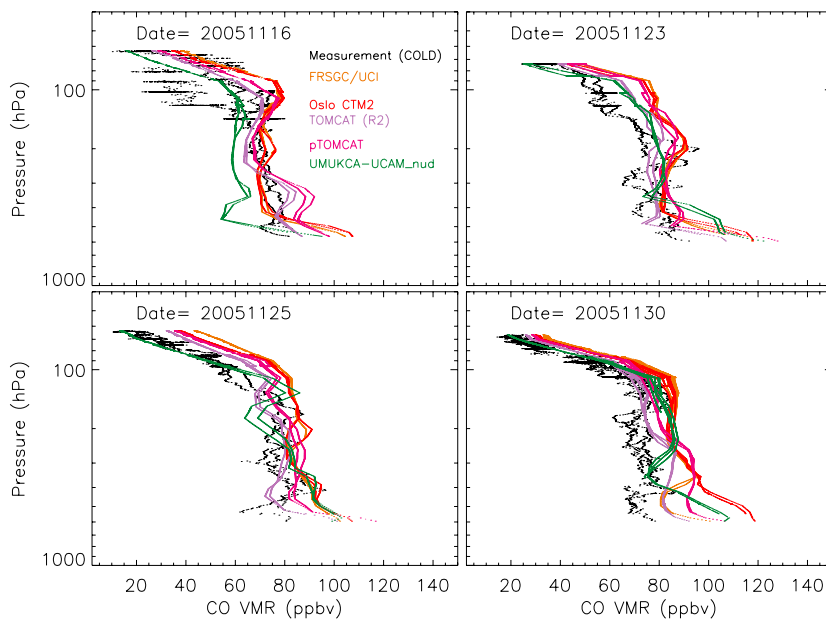


Fig. 8. A comparison between modelled and measured CO mixing ratios along the Geophysica flight track for (clockwise): the 16th, 23rd, 25th and 30th of November 2005. The measurements were made during the SCOUT-O3 campaign in Darwin.

[Title Page](#)[Abstract](#)[Introduction](#)[Conclusions](#)[References](#)[Tables](#)[Figures](#)[◀](#)[▶](#)[◀](#)[▶](#)[Back](#)[Close](#)[Full Screen / Esc](#)[Printer-friendly Version](#)[Interactive Discussion](#)

Modelling tropical tracer transport

C. R. Hoyle et al.

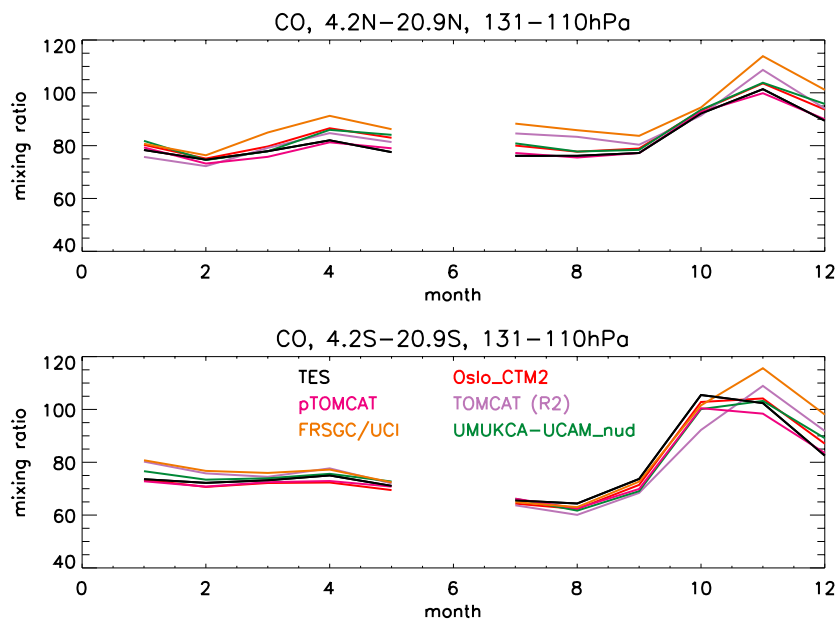


Fig. 9. A comparison between the monthly mean modelled CO mixing ratio in the northern (upper panel) and southern (lower panel) hemisphere upper tropical troposphere, and TES (Tropospheric Emission Spectrometer) satellite based measurements of CO.

[Title Page](#)[Abstract](#)[Introduction](#)[Conclusions](#)[References](#)[Tables](#)[Figures](#)[◀](#)[▶](#)[◀](#)[▶](#)[Back](#)[Close](#)[Full Screen / Esc](#)[Printer-friendly Version](#)[Interactive Discussion](#)